

# Longitudinal Modeling of Age-Dependent Latent Traits with Generalized Additive Latent and Mixed Models

Øystein Sørensen\*

Department of Psychology, University of Oslo  
and

Anders M. Fjell

Department of Psychology, University of Oslo

Department of Radiology and Nuclear Medicine, Oslo University Hospital  
and

Kristine B. Walhovd

Department of Psychology, University of Oslo

Department of Radiology and Nuclear Medicine, Oslo University Hospital

October 8, 2021

## Abstract

We present generalized additive latent and mixed models (GALAMMs) for analysis of clustered data with responses and latent variables depending smoothly on explanatory variables. An iterative profile likelihood algorithm is proposed, which combines existing efficient software for generalized additive mixed models with a quasi-Newton step. We derive asymptotic standard errors of both smooth and parametric terms. The models developed were motivated by applications in cognitive neuroscience, and three case studies are presented. First, we show how GALAMMs can successfully model the complex lifespan trajectory of latent episodic memory, using longitudinal data with five test scores at each timepoint. Next, we extend the model to study the joint trajectories of episodic and working memory across life. Finally, we study the effect of socioeconomic status on brain structure, using data on education and income together with hippocampal volumes estimated by magnetic resonance imaging. By combining semiparametric estimation with latent variable modeling, GALAMMs allow a more realistic representation of how brain and cognition vary across the lifespan, while simultaneously estimating latent traits from

---

\*The authors gratefully acknowledge the *European Research Council* under grant agreements 283634, 725025 (to A.M.F.) and 313440 (to K.B.W.), the *Norwegian Research Council* (to A.M.F., K.B.W.), *The National Association for Public Health's dementia research program, Norway* (to A.M.F) and center support from the *University of Oslo*

measured items. Simulation experiments suggest that model estimates are accurate even with moderate sample sizes.

*Keywords:* generalized additive mixed models, item response theory, latent variable modeling, cognitive neuroscience, structural equation modeling.

# 1 Introduction

Generalized linear mixed models (GLMMs) and nonlinear mixed models are widely used whenever observations can be divided into meaningful clusters. However, they require the parametric form of the effects to be exactly specified, and in many applications this may be impractical or not possible. For example, when studying how the human brain changes over the lifespan, volumes of different brain regions exhibit distinctive trajectories, differing with respect to rate of increase during childhood, age at which maximum is attained, and rate of decline in old age (Sørensen et al. 2021). Similarly, domain-specific cognitive abilities follow unique lifespan trajectories, with traits like episodic memory and processing speed reaching a peak in the early adulthood, while acquired knowledge like vocabulary peaks in late adulthood (McArdle et al. 2002). Generalized additive mixed models (GAMMs) (Wood 2017) flexibly estimate nonlinear relationships by a linear combination of known basis functions subject to smoothing penalty, and are ideally suited to these applications.

Both GLMMs and GAMMs can be used for analyzing multivariate response data, allowing estimation of correlated change across multiple processes. However, when multivariate responses are considered noisy realizations of lower-dimensional latent variables, GLMMs and GAMMs essentially assume a parallel measurement model (Novick 1966), in which the coefficients relating latent to observed variables are known at fixed values. Structural equation models (SEMs) offer more flexible latent variable modeling, and extensions of the SEM framework include nonlinear models (Arminger & Muthén 1998, Lee & Zhu 2000), semiparametric latent basis models (Meredith & Tisak 1990), and models for categorical and ordinal response data (Muthén 1984). Despite these advances, SEMs have limitations in terms of incorporating explanatory variables and analyzing unbalanced or multilevel data. Several proposed models bring SEMs closer to the flexibility of GLMMs, while retaining their ability to model latent variables (Mehta & Neale 2005, Muthén 2002, Oud & Jansen 2000, Proust-Lima et al. 2013, Rabe-Hesketh et al. 2004). In particular, generalized linear latent and mixed models (GLLAMMs) (Rabe-Hesketh et al. 2004) exploit the equivalence between random effects and latent variables to model latent and explanatory variables varying at any level. GLLAMMs are nonlinear hierarchical models whose likelihood function can be estimated with numerical integration (Rabe-Hesketh et al. 2005), and many special cases of GLLAMMs can be computed with a profile likelihood approach combining existing GLMM software with a general purpose optimization routine (Jeon & Rabe-Hesketh 2012). As GLLAMMs model the observed responses with an exponential family distribution, they are not limited to factor analytic measurement models, and contain important psychometric methods like item response models and latent class models as special cases.

While nonlinear modeling is straightforward with GLLAMMs, as with GLMMs the functional parametric forms are assumed known. In this paper, we introduce generalized additive latent and mixed models (GALAMMs), a semiparametric extension of GLLAMMs in which both the linear predictor and latent variables may depend smoothly on observed variables. Utilizing the mixed model view of smoothing (Ruppert et al. 2003, Wood 2017), we show that any GALAMM can be represented as a GLLAMM, with smoothing parameters estimated by maximum likelihood. This allows profile likelihood estimation of GALAMMs, combining existing GAMM software with a general purpose optimization routine. Asymptotic standard errors and confidence bands of estimated smooth functions can

be computed by extending existing methods for GAMMs (Marra & Wood 2012, Ruppert et al. 2003). The proposed methods are similar to fully Bayesian approaches to semi-parametric latent variable modeling (e.g., Fahrmeir & Raach (2007), Song et al. (2013)), all of which have been limited to latent variables varying at a single level. In contrast, GALAMMs allow multilevel modeling with any number of levels, and both nested and crossed random effects.

## 2 Generalized Additive Latent and Mixed Models

We consider multilevel models with components varying at  $L$  levels, and use generalized random coefficient notation (Skrondal & Rabe-Hesketh 2004, Ch. 4), which is here briefly reviewed. The multivariate responses for all units are stacked in a vector  $\mathbf{y}$  of length  $n$ , whose elements  $y_i$  are the elementary units of observation, varying at level 1. Latent variables vary at level 2 or higher, and  $\boldsymbol{\eta}^{(l)}$  denotes a vector of  $M_l$  latent variables varying at level  $l$ , with  $m$ th element  $\eta_m^{(l)}$ . The vector of all latent variables belonging to the  $j$ th level-2 unit is

$$\boldsymbol{\eta}_j = \left[ \boldsymbol{\eta}_{jk\dots z}^{(2)'} , \boldsymbol{\eta}_{k\dots z}^{(3)'} , \dots , \boldsymbol{\eta}_z^{(L)'} \right]', \quad (1)$$

and  $\boldsymbol{\eta}_j^{(l+)} = (\boldsymbol{\eta}_{\dots z}^{(l)'} , \dots , \boldsymbol{\eta}_z^{(L)'})'$  denotes elements of  $\boldsymbol{\eta}_j$  varying at level  $l$  or higher. Similarly,  $\mathbf{w}_j$  denotes explanatory variables on which the latent variables depend, and we assume these variables are permuted in such a way that we can write

$$\mathbf{w}_j = \left[ \mathbf{w}_{jk\dots z}^{(2)'} , \mathbf{w}_{k\dots z}^{(3)'} , \dots , \mathbf{w}_z^{(L)'} \right]', \quad (2)$$

where  $\mathbf{w}_{jk\dots z}^{(2)}$  are variables varying at level 2,  $\mathbf{w}_{k\dots z}^{(3)}$  are variables varying at level 3, and so on. Whereas latent variables are required at all levels, any element in (2) may be empty.

### 2.1 Model Framework

We assume a response distribution given by an exponential family with density

$$f(y_i | \theta_i, \phi) = \exp [\{y_i \theta_i - b(\theta_i)\} / \phi + c(y_i, \phi)], \quad (3)$$

where  $\theta_i$  is a function of the mean  $\mu_i = g^{-1}(\nu_i)$ ,  $g^{-1}(\cdot)$  being the inverse of link function  $g(\cdot)$ , and  $\nu_i$  a linear predictor. The linear predictor for level-1 unit  $i$  is related to explanatory variables  $\mathbf{x}_i$  and latent variables through the measurement model

$$\nu_i = \sum_{s=1}^S f_s(\mathbf{x}_i) + \sum_{l=2}^L \sum_{m=1}^{M_l} \eta_m^{(l)} \mathbf{z}_{mi}^{(l)'} \boldsymbol{\lambda}_m^{(l)}, \quad (4)$$

where  $\{f_s(\mathbf{x}_i)\}_{s=1}^S$  are functions of one or more elements of explanatory variables  $\mathbf{x}_i$ . We omit higher-level subscripts, but note that  $\eta_m^{(l)}$  is an element of  $\boldsymbol{\eta}_j$  in (1) varying at level  $l$ , with  $j$  denoting the level-2 unit to which the  $i$ th level-1 unit belongs. The term  $\mathbf{z}_{mi}^{(l)'} \boldsymbol{\lambda}_m^{(l)}$  relates the  $m$ th latent variable at level  $l$  to the  $i$ th measurement, where  $\boldsymbol{\lambda}_m^{(l)}$  contains

parameters to be estimated and  $\mathbf{z}_{mi}^{(l)}$  are explanatory variables varying at level  $l$  or higher. Each function  $f_s(\cdot)$  in (4) is a linear combination of  $B_s$  basis functions

$$f_s(\mathbf{x}_i) = \sum_{k=1}^{B_s} \omega_{ks} b_{ks}(\mathbf{x}_i), \quad s = 1, \dots, S, \quad (5)$$

with weights  $\omega_{ks}$ . The basis functions are assumed to be cubic regression splines or thin-plate regression splines (Wood 2003), and we assume multivariate smooth functions are constructed according to Wood et al. (2013).

The structural part of the model is

$$\boldsymbol{\eta}_j = \mathbf{B}\boldsymbol{\eta}_j + \mathbf{h}(\mathbf{w}_j) + \boldsymbol{\zeta}_j, \quad (6)$$

where  $\mathbf{B}$  is an  $M \times M$  matrix of coefficients for regressions between the latent variables, with  $M = \sum_{l=2}^L M_l$ . Following Rabe-Hesketh et al. (2004) we assume non-recursive relations between latent variables, and require that a latent variable varying at level  $l$  can only depend on latent variables varying at level  $l$  or higher. By a permutation of the latent variables varying at each level, it follows that  $\mathbf{B}$  is strictly upper diagonal (Skrondal & Rabe-Hesketh 2004, p. 109). We have also defined the vector valued function  $\mathbf{h}(\mathbf{w}_j)$ , itself composed of  $L - 1$  vector-valued functions  $\mathbf{h}_l\{\mathbf{w}_j^{(l+)}\}$  with  $M_l$  elements, one for each latent variable varying at level  $l$ :

$$\mathbf{h}(\mathbf{w}_j) = \begin{bmatrix} \mathbf{h}_2 \left\{ \mathbf{w}_j^{(2+)} \right\} \\ \mathbf{h}_3 \left\{ \mathbf{w}_j^{(3+)} \right\} \\ \vdots \\ \mathbf{h}_L \left\{ \mathbf{w}_j^{(L)} \right\} \end{bmatrix}, \quad \text{with } \mathbf{h}_l \left\{ \mathbf{w}_j^{(l+)} \right\} = \begin{bmatrix} h_{l1} \left\{ \mathbf{w}_j^{(l+)} \right\} \\ h_{l2} \left\{ \mathbf{w}_j^{(l+)} \right\} \\ \vdots \\ h_{l,M_l} \left\{ \mathbf{w}_j^{(l+)} \right\} \end{bmatrix}, \quad l = 2, \dots, L,$$

where  $h_{lm}\{\mathbf{w}_j^{(l+)}\}$  is a smooth function of a subset of  $\mathbf{w}_j^{(l+)}$  predicting the value of  $\eta_m^{(l)}$ . By this definition, latent variables varying at level  $l$  may only depend on explanatory variables varying at level  $l$  or higher. Each  $h_{lm}(\cdot)$  is a linear combination of  $D_{lm}$  basis functions  $d_{klm}(\cdot)$ ,

$$h_{lm} \left\{ \mathbf{w}_j^{(l+)} \right\} = \sum_{k=1}^{D_{lm}} \kappa_{klm} d_{klm} \left\{ \mathbf{w}_j^{(l+)} \right\}, \quad (7)$$

with weights  $\kappa_{klm}$ . If  $\eta_m^{(l)}$  does not depend on explanatory variables, we set  $D_{lm} = 0$ , and if  $\eta_m^{(l)}$  depends on  $S_{lm} > 1$  smooth functions it can be extended to  $\sum_{s=1}^{S_{lm}} h_{slm}(\cdot)$ , but we omit this for ease of exposition. To complete the specification of the structural model (6),  $\boldsymbol{\zeta}_j$  is a vector of normally distributed disturbances,  $\boldsymbol{\zeta}_j \sim N(\mathbf{0}, \boldsymbol{\Psi})$ , with block-diagonal covariance matrix  $\boldsymbol{\Psi} = \text{diag}(\boldsymbol{\Psi}^{(2)}, \dots, \boldsymbol{\Psi}^{(L)})$ ,  $\boldsymbol{\Psi}^{(l)}$  being the covariance of disturbances at level  $l$ .

In Supplement A, we show that any  $L$ -level GALAMM defined by (3), (4), and (6) can be transformed to a GLLAMM with  $L + 1$  levels, where the latent variables at the top level are inverse smoothing parameters for the functions defined in (5) and (7).

## 2.2 Reduced Form

Since  $\mathbf{B}$  is strictly upper diagonal,  $\mathbf{I} - \mathbf{B}$  is invertible and we can solve the structural model (6) for  $\boldsymbol{\eta}_j$  to get

$$\boldsymbol{\eta}_j = (\mathbf{I} - \mathbf{B})^{-1} \{ \mathbf{h}(\mathbf{w}_j) + \boldsymbol{\zeta}_j \} = \mathbf{C} \{ \mathbf{h}(\mathbf{w}_j) + \boldsymbol{\zeta}_j \}, \quad (8)$$

where we define the  $M \times M$  matrix  $\mathbf{C} = (\mathbf{I} - \mathbf{B})^{-1}$  and let  $c_{i,j}$  denote the element in its  $i$ th row and  $j$ th column. Let  $\pi_2(l, m)$  denote a function which takes as arguments the level  $l$  and index  $m$  of a latent variable  $\eta_m^{(l)}$ , and returns its position in the full latent variable vector  $\boldsymbol{\eta}$  defined in (1). With properly permuted indices,  $\pi_2(l, m) = m + \sum_{\tilde{l}=1}^{l-1} M_{\tilde{l}}$ . It follows from (8) that the scalar form of the structural model (6) is

$$\eta_{mj}^{(l)} = \sum_{\tilde{l}=2}^L \sum_{\tilde{m}=1}^{M_{\tilde{l}}} c_{\pi_2(l,m), \pi_2(\tilde{l}, \tilde{m})} \left[ h_{\tilde{l}\tilde{m}} \left\{ \mathbf{w}_j^{(\tilde{l}+)} \right\} + \zeta_{\tilde{m}j}^{(\tilde{l})} \right], \quad l = 2, \dots, L, \quad m = 1, \dots, M_l, \quad (9)$$

where we now use index  $j$  to make it explicit that  $\eta_{mj}^{(l)}$  is the value of the  $m$ th latent variable varying at level  $l$  for the  $j$ th level-2 unit, and similarly for the disturbance term  $\zeta_{mj}^{(l)}$ . Plugging (9) into the measurement model (4) gives the reduced form

$$\nu_i = \sum_{s=1}^S f_s(\mathbf{x}_i) + \sum_{l=2}^L \sum_{m=1}^{M_l} \left\{ \mathbf{z}_{mi}^{(l)'} \boldsymbol{\lambda}_m^{(l)} \right\} \sum_{\tilde{l}=2}^L \sum_{\tilde{m}=1}^{M_{\tilde{l}}} c_{\pi_2(l,m), \pi_2(\tilde{l}, \tilde{m})} \left[ h_{\tilde{l}\tilde{m}} \left\{ \mathbf{w}_j^{(\tilde{l}+)} \right\} + \zeta_{\tilde{m}j}^{(\tilde{l})} \right], \quad (10)$$

where the parameters to be estimated are  $\boldsymbol{\lambda}_m^{(l)}$ ,  $c_{m,\tilde{m}}$ , and the weights  $\omega_{ks}$  in  $f_s(\mathbf{x}_i)$  and  $\kappa_{klm}$  in  $h_{lm} \left\{ \mathbf{w}_j^{(l)} \right\}$ . The regression coefficients between latent variables can be converted back to their original form from the estimates of  $c_{m,\tilde{m}}$  through the transformation  $\mathbf{B} = \mathbf{I} - \mathbf{C}^{-1}$ .

In terms of the mixed model formulation in Supplement A we can derive the equivalent reduced form

$$\nu_i = \mathbf{x}_i' \boldsymbol{\beta} + \sum_{\tilde{l}=2}^{L+1} \sum_{\tilde{m}=1}^{M_{\tilde{l}}} \sum_{l=2}^{L+1} \sum_{m=1}^{M_l} \left\{ \mathbf{z}_{mi}^{(l)'} \boldsymbol{\lambda}_m^{(l)} \right\} c_{\pi(l,m), \pi(\tilde{l}, \tilde{m})} \left\{ \boldsymbol{\Gamma}_{\pi_2(l,m), \cdot} \mathbf{w}_j + \zeta_{\tilde{m}j}^{(\tilde{l})} \right\}, \quad (11)$$

where  $\boldsymbol{\Gamma}_{j, \cdot}$  denotes the  $j$ th row of  $\boldsymbol{\Gamma}$  and hence  $\boldsymbol{\Gamma}_{\pi_2(l,m), \cdot} \mathbf{w}_j$  is a scalar.

## 2.3 Profile Likelihood Estimation

The reduced form (11) is a nonlinear mixed model containing products of fixed effects as well as products between fixed and random effects, and the linear predictor is in general linked to the observed outcome with a nonlinear link function. We now describe an extension of the profile likelihood approach proposed by Jeon & Rabe-Hesketh (2012) for maximum likelihood estimation of GALAMMs defined by (4) and (6). The algorithm combines existing GAMM software with a general purpose optimization routine. Since the conversion to mixed model representation is performed automatically by the GAMM software, we derive the method from the reduced form (10).

Assume estimates  $\hat{\boldsymbol{\lambda}}_m^{(l)}$  and  $\hat{c}_{\pi(l,m),\pi(\tilde{l},\tilde{m})}$  are available, and fix  $\boldsymbol{\lambda}_m^{(l)}$  and  $c_{\pi(l,m),\pi(\tilde{l},\tilde{m})}$  in (10) to these values to get

$$\nu_i = \sum_{s=1}^S f_s(\mathbf{x}_i) + \sum_{\tilde{l}=2}^L \sum_{\tilde{m}=1}^{M_{\tilde{l}}} \sum_{l=2}^L \sum_{m=1}^{M_l} \left\{ \mathbf{z}_{mi}^{(l)'} \hat{\boldsymbol{\lambda}}_m^{(l)} \right\} \hat{c}_{\pi(l,m),\pi(\tilde{l},\tilde{m})} \left[ h_{\tilde{l}\tilde{m}} \left\{ \mathbf{w}_j^{(\tilde{l}+)} \right\} + \zeta_{\tilde{m}j}^{(\tilde{l})} \right], \quad (12)$$

which can be recognized as a GAMM. The first term on the right-hand side contains  $S$  smooth terms  $f_s(\mathbf{x}_i)$ . Expanding the square brackets, the second term contains  $M$  varying-coefficient terms (Hastie & Tibshirani 1993) of the form

$$h_{\tilde{l}\tilde{m}} \left\{ \mathbf{w}_j^{(\tilde{l}+)} \right\} \sum_{l=2}^L \sum_{m=1}^{M_l} \left\{ \mathbf{z}_{mi}^{(l)'} \hat{\boldsymbol{\lambda}}_m^{(l)} \right\} \hat{c}_{\pi(l,m),\pi(\tilde{l},\tilde{m})}, \quad \tilde{l} = 2, \dots, L, \quad \tilde{m} = 1, \dots, M_{\tilde{l}}.$$

It may help intuition to consider the case with no regressions between latent variables, for which  $\mathbf{C} = (\mathbf{I} - \mathbf{0})^{-1} = \mathbf{I}$  and the varying-coefficient terms simplify to

$$\mathbf{z}_{mi}^{(l)'} \hat{\boldsymbol{\lambda}}_m^{(l)} h_{lm} \left\{ \mathbf{w}_j^{(l+)} \right\}, \quad l = 2, \dots, L, \quad m = 1, \dots, M_l,$$

with  $h_{lm}(\cdot)$  now a smoothly varying regression coefficient for  $\mathbf{z}_{mi}^{(l)'} \hat{\boldsymbol{\lambda}}_m^{(l)}$ . The last term inside the square brackets in (12) contains  $M$  random effects.

Let  $\Theta$  denote the set of all parameters of the GALAMM in mixed model formulation (Supplement A), including random coefficients varying at level  $L + 1$ . Defining  $\boldsymbol{\Lambda}^{(l)} = [\boldsymbol{\lambda}_1^{(l)} \dots \boldsymbol{\lambda}_{M_l}^{(l)}]$  and  $\boldsymbol{\Lambda} = [\boldsymbol{\Lambda}^{(2)} \dots \boldsymbol{\Lambda}^{(L)}]$ , we divide  $\Theta$  into  $\Theta_1 = \{\boldsymbol{\Lambda}, \mathbf{B}\}$  and  $\Theta_2$  containing all remaining parameters. We similarly define the likelihood as a function of these two parameter sets  $L(\Theta) = L(\Theta_1, \Theta_2)$ . Let

$$\hat{\Theta}_2(\Theta_1) = \underset{\Theta_2}{\operatorname{argmax}} L(\Theta_1, \Theta_2), \quad (13)$$

define the maximum likelihood estimates of the parameters in  $\Theta_2$  as a function of the parameters in  $\Theta_1$ , and define the profile likelihood

$$L(\Theta_1) = \max_{\Theta_2} L(\Theta_1, \Theta_2) = L\left\{\Theta_1, \hat{\Theta}_2(\Theta_1)\right\}. \quad (14)$$

Equations (13) and (14) can be iterated to obtain the maximum likelihood estimates of  $\Theta$ . In the inner step, (13) is computed at  $\Theta_1$  by solving the GAMM (12) after plugging in values of  $\hat{\boldsymbol{\lambda}}_m$  and  $\hat{c}_{\pi(l,m),\pi(\tilde{l},\tilde{m})}$  from  $\Theta_1$ . In the outer step,  $L(\Theta_1)$  is maximized with respect to  $\Theta_1$ . Convergence is achieved when changing  $\Theta_1$  along any of its dimensions no longer leads to an increase in  $L(\Theta_1)$ .

For fixed values of  $\hat{\Theta}_1$ , R packages 'mgcv' (Wood 2017) and 'gamm4' (Wood & Scheipl 2020) solve (13) efficiently. While 'gamm4' uses 'lme4' (Bates et al. 2015) to solve the underlying GLMM with a full Laplace approximation, the `gamm` function in 'mgcv' uses the 'nlme' package (Pinheiro et al. 2020) for Gaussian models with unit link and `glmmPQL` from the 'MASS' package (Venables & Ripley 2002) otherwise. As the latter uses penalized quaslikelihood (Breslow & Clayton 1993, Schall 1991), maximum likelihood estimates are not obtained, and hence 'gamm4' will typically be preferable in the generalized case.

The profile likelihood (14) can be maximized with a general purpose optimization routine, using the log likelihood of the GAMM (13) as objective function. In our experiments, both the Nelder-Mead algorithm (Nelder & Mead 1965) and the limited-memory Broyden-Fletcher-Goldfarb-Shanno algorithm with box constraints (L-BFGS-B) (Byrd et al. 1995) have achieved stable and good performance, with the latter typically being faster. While Nelder-Mead is derivative free, L-BFGS-B also uses the gradient of the log likelihood with respect to  $\Theta_1$  when maximizing (14), which can be obtained using finite differences.

## 2.4 Standard Errors

Let  $\hat{\Theta} = (\hat{\Theta}_1, \hat{\Theta}_2)$  denote the estimates obtained by profile likelihood estimation. The Fisher information matrix  $\mathbf{I}(\hat{\Theta}_1, \hat{\Theta}_2)$  and its inverse can be defined by

$$\mathbf{I}(\hat{\Theta}_1, \hat{\Theta}_2) = \begin{bmatrix} \mathbf{I}_{(\hat{\Theta}_1, \hat{\Theta}_1)} & \mathbf{I}_{(\hat{\Theta}_1, \hat{\Theta}_2)} \\ \mathbf{I}_{(\hat{\Theta}_2, \hat{\Theta}_1)} & \mathbf{I}_{(\hat{\Theta}_2, \hat{\Theta}_2)} \end{bmatrix} \text{ and } \mathbf{I}^{-1}(\hat{\Theta}_1, \hat{\Theta}_2) = \begin{bmatrix} \mathbf{C}_{(\hat{\Theta}_1, \hat{\Theta}_1)} & \mathbf{C}_{(\hat{\Theta}_1, \hat{\Theta}_2)} \\ \mathbf{C}_{(\hat{\Theta}_2, \hat{\Theta}_1)} & \mathbf{C}_{(\hat{\Theta}_2, \hat{\Theta}_2)} \end{bmatrix}.$$

The block  $\mathbf{C}_{(\hat{\Theta}_1, \hat{\Theta}_1)}$  is the covariance matrix of  $\hat{\Theta}_1$  taking uncertainty in  $\hat{\Theta}_2$  into account, and is readily obtained from the profile likelihood algorithm (13)–(14) as minus the inverse of the Hessian evaluated at the final estimates of  $\hat{\Theta}_1$  (Jeon & Rabe-Hesketh 2012). The covariance matrix obtained when solving (13) corresponds to  $\mathbf{I}_{(\hat{\Theta}_2, \hat{\Theta}_2)}^{-1}$  and does not take uncertainty in  $\hat{\Theta}_1$  into account. Following Parke (1986), Jeon & Rabe-Hesketh (2012) defined the asymptotic covariance matrix of  $\hat{\Theta}_2$  as

$$\text{Cov}(\hat{\Theta}_2, \hat{\Theta}_2) = \mathbf{I}_{(\hat{\Theta}_2, \hat{\Theta}_2)}^{-1} + \left[ \frac{\partial \hat{\Theta}_2(\Theta_1)}{\partial \Theta_1} \Bigg|_{\Theta_1 = \hat{\Theta}_1} \right] \mathbf{C}_{(\hat{\Theta}_1, \hat{\Theta}_1)} \left[ \frac{\partial \hat{\Theta}_2(\Theta_1)}{\partial \Theta_1} \Bigg|_{\Theta_1 = \hat{\Theta}_1} \right]'. \quad (15)$$

It also follows from Parke (1986) that

$$\text{Cov}(\hat{\Theta}_1, \hat{\Theta}_2) = \text{Cov}(\hat{\Theta}_2, \hat{\Theta}_1)' = \mathbf{C}_{(\hat{\Theta}_1, \hat{\Theta}_1)} \left[ \frac{\partial \hat{\Theta}_2(\Theta_1)}{\partial \Theta_1} \Bigg|_{\Theta_1 = \hat{\Theta}_1} \right]', \quad (16)$$

which lets us define the full asymptotic covariance matrix of  $\Theta$  as

$$\text{Cov}(\hat{\Theta}) = \begin{bmatrix} \mathbf{C}_{(\hat{\Theta}_1, \hat{\Theta}_1)} & \text{Cov}(\hat{\Theta}_1, \hat{\Theta}_2) \\ \text{Cov}(\hat{\Theta}_2, \hat{\Theta}_1) & \text{Cov}(\hat{\Theta}_2, \hat{\Theta}_2) \end{bmatrix}. \quad (17)$$

With a one-sided finite difference scheme, the Jacobian  $\partial \hat{\Theta}_2(\Theta_1)/\partial \Theta_1$  in (15) and (16) requires computing the GAMM (13) once for each element of  $\Theta_1$ , and since the derivative with respect to each component of  $\Theta_1$  can be computed independently, we recognize this as a perfectly parallel problem.

Asymptotic standard errors of parametric components are obtained from the corresponding elements of  $\text{Cov}(\hat{\Theta})$ . Standard errors for smooth terms, or for prediction in general, requires consideration of multiple elements of  $\text{Cov}(\hat{\Theta})$ . For example, consider the function  $f_s(\mathbf{x}_i)$  in equation (5), define  $\hat{\mathbf{X}}_s$  as in Supplement A, eq. (1), let  $\hat{\omega}_s \subset \hat{\Theta}_2$  be the vector of estimated weights, and  $\text{Cov}(\hat{\omega}_s)$  a submatrix of  $\text{Cov}(\hat{\Theta})$  restricted to the columns



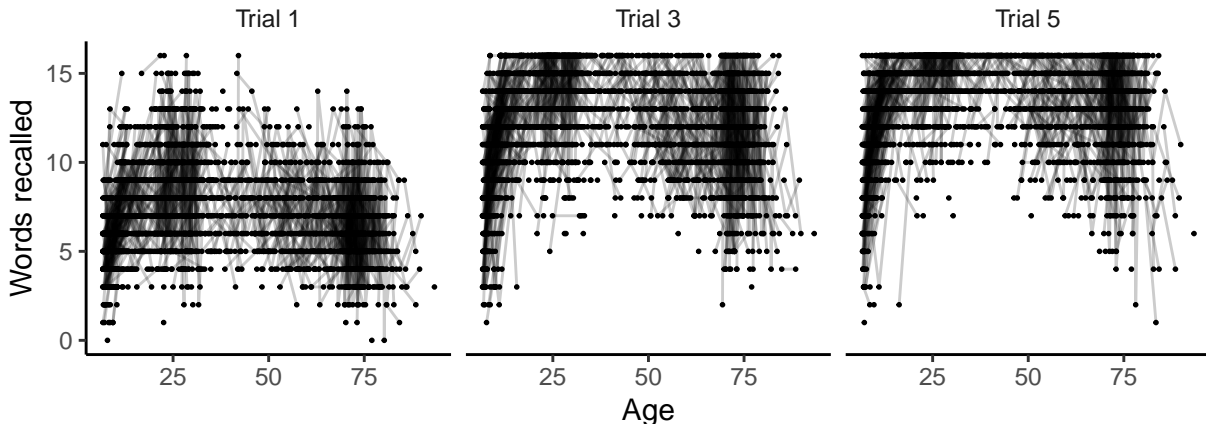


Figure 1: Observed responses to three of the five CVLT items. Dots show individual responses, and black lines connect multiple timepoints for the same participant.

corresponding to  $\hat{\omega}_s$ . The estimate of this smooth term equals  $\hat{\mathbf{f}}_s = \tilde{\mathbf{X}}_s \hat{\omega}_s$ , and defining  $\mathbf{v}_s = \text{diag}(\tilde{\mathbf{X}}_s \text{Cov}(\hat{\omega}_s) \tilde{\mathbf{X}}_s')$ , the standard error at the  $i$ th evaluation point is  $\sqrt{v_{si}}$ , the  $i$ th element of  $\mathbf{v}_s$ . Approximate pointwise confidence intervals over the evaluation points are given by  $f_{si} \pm z_{\alpha/2} \sqrt{v_{si}}$ , where  $z_{\alpha/2}$  is the  $\alpha/2$  quantile of the standard normal distribution (Wood 2017, Chapter 6.10). Confidence intervals constructed this way have approximately  $(1 - \alpha)100\%$  coverage averaged over the domain of the function (Marra & Wood 2012). In contrast, simultaneous confidence intervals which cover the function over its whole domain with probability  $(1 - \alpha)100\%$  require a critical value  $\tilde{z}_{\alpha/2} \geq z_{\alpha/2}$ . An estimate of  $\tilde{z}_{\alpha/2}$  can be obtained by sampling from the empirical Bayes posterior distribution of  $f_s(\cdot)$ , and finding the quantile for which  $(1 - \alpha)100\%$  of the sampled curves are completely confined within  $f_{si} \pm \tilde{z}_{\alpha/2} \sqrt{v_{si}}$  (Ruppert et al. 2003, Chapter 6.5).

### 3 Case Studies

We now present three case studies highlighting how GALAMMs can be used to address open problems in cognitive neuroscience, all using data from the Center for Lifespan Changes in Brain and Cognition (LCBC) (Fjell et al. 2018, Walhovd et al. 2016). Each application is accompanied by a simulation study (described in Supplement B) in which the data structure and model parameters closely mimicked the real data.

#### 3.1 Latent Response Models: Estimating the Lifespan Trajectory of Episodic Memory

The California verbal learning test (CVLT) (Delis et al. 2000) is a widely used test of episodic memory. During the test, the experimenter reads a list of 16 words aloud, and subsequently the participant is asked to repeat the words back. This procedure is repeated in five trials. Our dataset consisted of CVLT scores from 3470 observations of 1850 healthy participants between 6 and 93 years of age. Each participant completed the test between 1

and 6 times, and the time interval between two consecutive measurements varied between 5 weeks and 9.7 years, with mean interval 2.4 years. We defined the number of successes in a single trial as level-1 units, so each timepoint for a given participant was a level-2 unit. As all participants had completed the full CVLT at each timepoint, each level-2 unit contained five level-1 units. The level-3 units were individual participants, containing between 1 and 6 level-2 units. Figure 1 shows that the number of words recalled varied nonlinearly across the lifespan, with a rapid increase during childhood, stability during adulthood, and decrease in old age. The participants recalled a larger number of words in the later trials, illustrating a within-timepoint learning effect. Ceiling effects were also apparent in later trials, as a large number of participants remembered all 16 words.

Assuming that the number of words recalled are noisy measurements of the participants' episodic memory, our goal was to estimate how episodic memory varies with age. We defined a three-level GALAMM with binomially distributed level-1 responses  $y_i \in \{0, \dots, 16\}$ , using a logit link  $\nu_i = g(\mu_i) = \log\{\mu_i/(1-\mu_i)\}$  where  $\mu_i$  was the expected proportion of successes. The measurement model and structural model took the form

$$\nu_i = \mathbf{d}'_{ti}\boldsymbol{\beta}_t + d_{ri}\beta_r + \mathbf{d}'_{ti}\boldsymbol{\lambda} \sum_{l=2}^3 \eta^{(l)} \quad (18)$$

$$\boldsymbol{\eta}_j = \begin{bmatrix} \eta_{jk}^{(2)} \\ \eta_k^{(3)} \end{bmatrix} = \begin{bmatrix} h(w_{jk}) \\ 0 \end{bmatrix} + \begin{bmatrix} \zeta_{jk}^{(2)} \\ \zeta_k^{(3)} \end{bmatrix}, \quad (19)$$

where unnecessary subscripts and superscripts are omitted.  $\mathbf{d}_{ti}$  was an indicator vector whose  $k$ th element equaled one if the  $i$ th level-1 unit was a measurement of CVLT trial  $k$  and zero otherwise, and  $\boldsymbol{\beta}_t = (\beta_{t1}, \dots, \beta_{t5})'$  was a vector of item effects. Retest effects, which can be defined as the marginal effect of having taken the CVLT previously (Woods et al. 2006), were accounted for by the variable  $d_{ri} \in \{0, 1\}$  indicating whether the participant had taken the test previously at the given timepoint. The latent episodic memory  $\eta_{jk}^{(2)}$  at timepoint  $j$  of participant  $k$  had a systematic component  $h(w_{jk})$ , which was a smooth function of age  $w_{jk}$ , and a random intercept  $\zeta_{jk}^{(2)}$  varying between timepoints of a given participant. The smooth function was specified following (7),  $h(w_{jk}) = \sum_{k=1}^D \kappa_k d(w_{jk})$  with  $D = 15$  cubic regression splines and squared second derivative penalization. The latent variable  $\eta_k^{(3)} = \zeta_k^{(3)}$  was a random intercept varying between participants and random intercepts at each level were assumed normally distributed with mean zero, i.e.,  $\boldsymbol{\zeta} \sim N(\mathbf{0}, \boldsymbol{\Psi})$  where  $\boldsymbol{\Psi} = \text{diag}(\psi^{(2)}, \psi^{(3)})$ . The constraints  $\mathbf{z}_i^{(2)} = \mathbf{z}_i^{(3)} = \mathbf{d}_{ti}$  and  $\boldsymbol{\lambda}^{(2)} = \boldsymbol{\lambda}^{(3)} = \boldsymbol{\lambda}$  implicit in (18) ensure that  $\eta_k^{(3)}$  can be interpreted as a random intercept for the latent level  $\eta_{jk}^{(2)}$  (Rabe-Hesketh et al. 2004, pp. 182–183). In the factor loadings  $\boldsymbol{\lambda} = (\lambda_1, \dots, \lambda_5)'$ , the constraint  $\lambda_1 = 1$  was imposed for identifiability. The smooth term  $h(w_{jk})$  was freely estimated, so the intercept for an item  $k \in \{1, \dots, 5\}$  was  $\beta_{tk} + \lambda_k h(0)$ , where  $\beta_{t1} = 0$  for identifiability.

Plugging (19) into (18) gives the reduced form

$$\nu_i = \mathbf{d}'_{ti}\boldsymbol{\beta}_t + d_{ri}\beta_r + h(w_{jk}) \mathbf{d}'_{ti}\boldsymbol{\lambda} + \zeta_{jk}^{(2)} \mathbf{d}'_{ti}\boldsymbol{\lambda} + \zeta_k^{(3)} \mathbf{d}'_{ti}\boldsymbol{\lambda}, \quad (20)$$

and inserting estimates  $\hat{\boldsymbol{\lambda}}$ , (20) is recognized as a GAMM with parametric terms  $\mathbf{d}'_{ti}\boldsymbol{\beta}_t + d_{ri}\beta_r$ , varying-coefficient term  $h(w_{jk})\mathbf{d}'_{ti}\hat{\boldsymbol{\lambda}}$ , and random effects  $\zeta_{jk}^{(2)}$  and  $\zeta_k^{(3)}$  of  $\mathbf{d}'_{ti}\hat{\boldsymbol{\lambda}}$ . Defining  $\Theta_1 = \{\boldsymbol{\lambda}\}$  and  $\Theta_2 = \{\boldsymbol{\omega}, \boldsymbol{\kappa}, \boldsymbol{\Psi}\}$ , this representation was used to solve (13) in the profile likelihood algorithm using 'gamm4' (Wood & Scheipl 2020), yielding estimates  $\hat{\Theta}_2 = \{\hat{\boldsymbol{\omega}}, \hat{\boldsymbol{\kappa}}, \hat{\boldsymbol{\Psi}}\}$

Table 1: Parameter estimates in latent response model. 'SE-naive' denotes standard error not taking uncertainty in factor loadings into account.

Parameter	Estimate	SE	SE-naive
<i>Item effects</i>			
$\beta_{t2}$	1.22	0.022	0.019
$\beta_{t3}$	2.05	0.031	0.026
$\beta_{t4}$	2.53	0.036	0.030
$\beta_{t5}$	2.89	0.040	0.032
<i>Retest effect</i>			
$\beta_r$	0.15	0.019	0.019

as a function of  $\Theta_1$ . Estimates  $\hat{\Theta}_1 = \{\hat{\lambda}\}$  were obtained by optimizing (14) with the L-BFGS-B algorithm (Byrd et al. 1995). The covariance matrix was estimated following Section 2.4, using the R package 'numDeriv' (Gilbert & Varadhan 2019) for calculation of Jacobians with a forward difference scheme. Very similar estimates were obtained with thin-plate regression splines (Wood 2003) and with  $D = 30$  cubic regression splines.

Estimates of regression coefficients are shown in Table 1. The item effects increased with trial number, reflecting that participants on average achieved higher scores in later trials, and for several items the asymptotic standard errors computed with (15) were substantially higher than the uncorrected standard errors. From the estimated retest effect and its standard error we find that the odds ratio for correctly recalling a word when having taken the test previously compared to not having taken the test previously is  $\exp(\beta_r) = 1.16$ . The variance components were estimated to  $\sqrt{\hat{\psi}^{(2)}} = 0.26$  and  $\sqrt{\hat{\psi}^{(3)}} = 0.28$ , indicating that conditional on the explanatory variables, a single participant's variation between timepoints was of comparable magnitude to the variation between participants.

Item characteristic curves show the probability of a correct response in trial  $k$  as a function of the latent level,  $f_k\{\eta^{(2)}\} = (1 + \exp[-\{\beta_{tk} + \lambda_k\eta^{(2)}\}])^{-1}$  (Skrondal & Rabe-Hesketh 2004, Ch. 3.3.4), and are shown in Figure 2 (left) together with estimates and standard errors of factor loadings. The curve for trial 1 equaled  $f_1\{\eta^{(2)}\} = [1 + \exp\{-\eta^{(2)}\}]^{-1}$  due to the identifiability restrictions imposed, and all other curves were defined relative to this one. The items' ability to discriminate between high and low levels of episodic memory increased from trial 1 to trial 5, and the increasingly positive item effects for trials 2-5 imply that the probability of correct response at the average level of episodic memory got increasingly close to 1. The estimated lifespan trajectory of episodic memory, Figure 2 (right), showed a steep increase during childhood until the age of around 18 followed by a period of stability during young adulthood, slow decline between the age of 35 and 75, and finally a steep decrease after the age of 75. Simultaneous confidence intervals required a critical value 3.06 at 95% confidence level, and are shown in light gray in Figure 2 (right).

The timing of age-related decline in cognitive function has received much focus, with cross-sectional studies indicating that the decline starts around the age of 20 (Salthouse 2009) and longitudinal studies showing a stable level until the age of 60 (Rönnlund et al. 2005). Debate has concerned the relative magnitude of cohort effect bias in cross-sectional studies versus retest effect bias in longitudinal studies (Nilsson et al. 2009, Raz & Lindenberger 2011, Salthouse 2009, Schaie 2009). When retest effects are properly accounted for

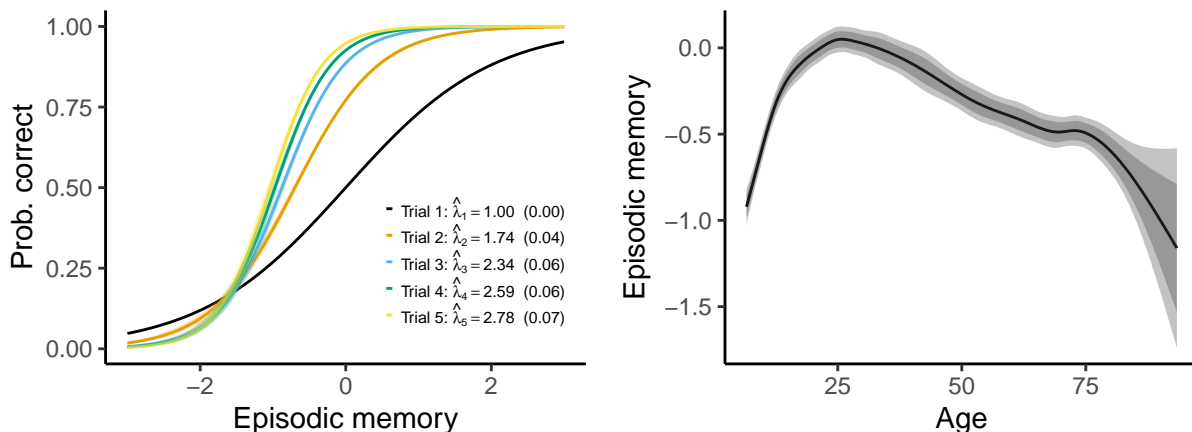


Figure 2: Left: Item response curves. Estimated factor loadings and standard errors are shown by the legend, and shaded regions show 95% confidence bands. Right: Estimate of lifespan episodic memory  $h(w)$ , with values on  $y$ -axis in units of  $\sqrt{\hat{\psi}^{(3)}}$ . Shaded regions shows 95% pointwise (dark gray) and simultaneous (light gray) confidence bands.

in longitudinal studies, the difference between the approaches is typically reduced (Tucker-Drob et al. 2019), suggesting that retest effects are larger than cohort effects. The trajectory in Figure 2 (right) shows some agreement with Salthouse (2009), but all the aforementioned studies used restrictive parametric models and are hence not directly comparable. The GALAMM-based model presented in this section offers the opportunity for more accurate estimation of lifespan cognitive development.

### 3.2 Factor-by-Curve Interaction Models: Joint Modeling of Episodic and Working Memory

Episodic memory, considered in Section 3.1, involves recollection of specific events. Working memory, on the other hand, involves the ability to hold information temporarily. Dating back at least to Spearman (1904), individual abilities in cognitive domains are known to be correlated, and we will here demonstrate how GALAMMs with multiple smooth terms can be used to model lifespan trajectories of cognitive abilities in multiple domains. In addition to CVLT, the data contained measurements of working memory assessed by digit span tests. In a digit span test, a sequence of numbers of increasing length is read out loud, and the final score is defined as the length of the longest list of numbers the participant was able to immediately repeat back (Blackburn & Benton 1959). In an additional test, the participants were instead asked to repeat the list of numbers backwards. Both experiments were repeated up to a list of length 16, which is the maximum possible score. The total sample consisted of 3763 timepoints for 1924 individuals, of which 1781 had both CVLT and digit span scores in at least one timepoint. The number of level-1 units was 24244. Figure 1 in Supplement C shows item responses to the digit span tests.

We modeled the maximum length of the lists recalled in the digit span forward and backward tests as binomially distributed variables with 16 trials, and could thus use a logistic link for both the digit span items and the CVLT items. Extending model (18)-(19)

we defined

$$\nu_i = \mathbf{d}'_{ti}\boldsymbol{\beta}_t + \mathbf{d}'_{ri}\boldsymbol{\beta}_r + \sum_{l=2}^3 \sum_{m=1}^2 \mathbf{d}'_{ti}\boldsymbol{\lambda}_m\eta_m^{(l)} \quad (21)$$

$$\boldsymbol{\eta} = \begin{bmatrix} \eta_1^{(2)} \\ \eta_2^{(2)} \\ \eta_1^{(3)} \\ \eta_2^{(3)} \end{bmatrix} = \begin{bmatrix} h_1(w) \\ h_2(w) \\ 0 \\ 0 \end{bmatrix} + \begin{bmatrix} \zeta_1^{(2)} \\ \zeta_2^{(2)} \\ \zeta_1^{(3)} \\ \zeta_2^{(3)} \end{bmatrix}. \quad (22)$$

In the measurement model (21),  $\mathbf{d}'_{ti}\boldsymbol{\beta}_t$  contained item effects, now also including digit span forward and backward. We modeled the retest effects separately, such that  $\mathbf{d}_{ri}$  now was a vector of size 2, whose first element was an indicator for the event that the participant had taken the CVLT at a previous time, and whose second element was a similar indicator for the digit span test. It follows that  $\boldsymbol{\beta}_r = (\beta_{r1}, \beta_{r2})'$  contained retest effects for the CVLT and digit span test, respectively. The first vector of factor loadings  $\boldsymbol{\lambda}_1 = (\lambda_{11}, \dots, \lambda_{15})'$  was defined as in the previous section, while the second vector  $\boldsymbol{\lambda}_2 = (\lambda_{21}, \lambda_{22})'$  contained loadings relating working memory to measured digit span. For identifiability, we set  $\lambda_{11} = \lambda_{21} = 1$ . In the structural model (22),  $h_1(w)$  and  $h_2(w)$  modeled episodic memory and working memory as smooth functions of age, each defined as the linear combination of ten cubic regression splines, with squared second derivative penalization. Since episodic and working memory are closely related, we defined these with factor-by-curve interaction models with a common smoothing parameter (Coull et al. 2001). In terms of the mixed model representation defined in Supplement A, dropping unnecessary indices, these smooth functions had only a random part

$$h_m = \mathbf{R}_m\boldsymbol{\eta}_m = \eta_{m1} + w\eta_{m2} + \mathbf{R}_{m3}\boldsymbol{\eta}_{m3}, \quad m = 1, 2,$$

with  $\eta_{m1} \sim N\{0, \psi_1^{(4)}\}$  a random intercept for the overall level,  $\eta_{m2} \sim N\{0, \psi_2^{(4)}\}$  a random linear slope, and  $\mathbf{R}_{m3}$  a matrix in the range space of the squared second derivative smoothing penalty, with  $\boldsymbol{\eta}_{m3} \sim N\{\mathbf{0}, \psi_3^{(4)}\mathbf{I}_8\}$  the corresponding random effect. The terms  $\zeta_1^{(2)}$  and  $\zeta_2^{(3)}$  in (22) were random intercepts for episodic and working memory, respectively, varying between timepoints for the same participant, while  $\zeta_1^{(3)}$  and  $\zeta_2^{(3)}$  were random intercepts varying between participants. Their covariance matrices were freely estimated. Since the structural model contained no constant fixed term, all seven items were explicitly represented in the item effect term  $\mathbf{d}'_{ti}\boldsymbol{\beta}_t$  in the measurement model.

The model was fitted following Section 3.1. The correlation between level-3 random intercepts  $\zeta_1^{(3)}$  and  $\zeta_2^{(3)}$  was estimated to 0.41, indicating that conditional on age, there was a fairly strong positive correlation between individual levels of episodic and working memory. This is slightly below a recent meta analysis of adult samples by Tucker-Drob et al. (2019) who found a level communality of 0.56 across a large range of cognitive domains. Surprisingly, the correlation of level-2 intercepts was estimated to 1.0, which at face value indicates that a person's deviation from her/his long-term level at any given day was identical across episodic and working memory. However, simulation experiments shown in Section 2 of Supplement B suggest that it is not possible to accurately estimate the level-2 correlation with the low number of timepoints per participant characteristic of these data, and we should hence not interpret it further.

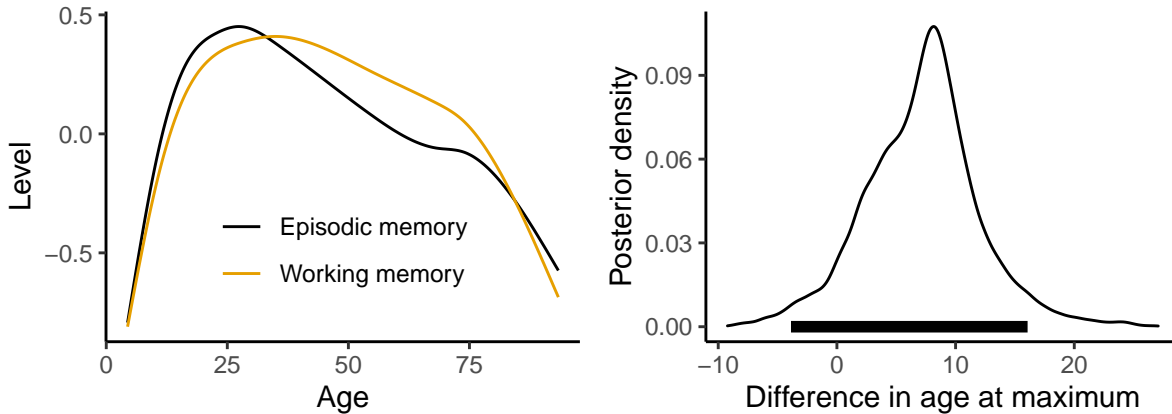


Figure 3: Left: Estimated lifespan trajectories of episodic and working memory. Right: Empirical Bayes posterior distribution of the difference in age at maximum of episodic and working memory. Horizontal bar denotes 95% highest posterior density interval.

Figure 3 (left) shows the estimated lifespan trajectories for episodic and working memory. We estimated the difference in age at maximum of the two curves by drawing 10000 random samples from the empirical Bayes posterior distributions of the spline weights, computing the trajectories on a dense grid between the age of 10 and 60, and recording the difference between the age at maximum working memory and the age at maximum episodic memory. Figure 3 (right) shows the posterior distribution of the difference, which had a mean of 7 years. A 95% highest posterior density interval, indicated by the horizontal bar at the bottom of the plot, spanned differences from -3.0 years to 16.7 years. It follows that we could not conclude from these data whether working memory peaked at a higher age than episodic memory. The ceiling effects apparent in the CVLT (Figure 1) but not in the digit span test (Supplement C, Figure 1) represents a potential confounding factor, as they may have lead to a large number of participants achieving a maximum score before their maximum latent level was reached.

### 3.3 Latent Covariates: Socioeconomic Status and Hippocampal Volume

The association between socioeconomic status and brain development has been the subject of much research. It has been proposed that higher socioeconomic status during childhood protects against late-life dementia (Livingston et al. 2017), whereas a meta-analysis found that the associations between socioeconomic status and brain structure varied considerably between samples (Walhovd et al. 2020). The hippocampus is a brain region which plays an important role in memory consolidation, and is one of the first regions to be damaged in Alzheimer’s disease (Dubois et al. 2016). Positive associations have been found between socioeconomic status and hippocampal volume in children (Noble et al. 2012), and between childhood socioeconomic status and adult brain size (Staff et al. 2012). However, while hippocampal volume is known to be a nonlinear function of age, most studies investigating the association have used linear regression analyses. An exception is Nyberg et al. (2021),

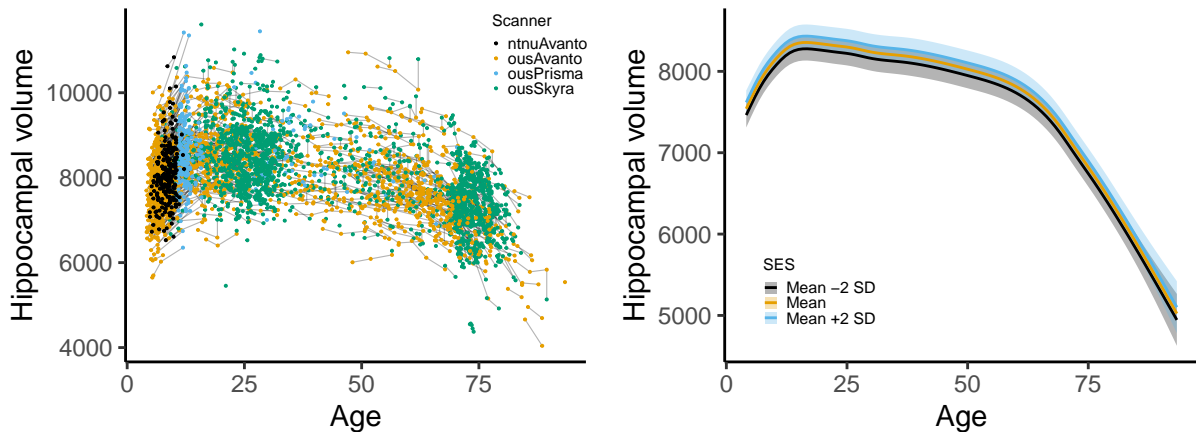


Figure 4: Left: Total volumes of left and right hippocampus (in  $\text{mm}^3$ ) plotted versus age. Repeated observations of the same individual are connected with gray lines. Right: Estimated hippocampal volume trajectories at mean socioeconomic status (SES) and at two standard deviation above or below mean. Shaded regions show 95% pointwise confidence intervals for SES two standard deviations above or below mean.

who used GAMMs to model the hippocampal trajectory, and found no relationship between longitudinal change in hippocampal volume and educational attainment in two large adult samples.

We here considered the association between hippocampal volume and socioeconomic status across the lifespan. Hippocampal volumes were estimated with FreeSurfer 7 (Fischl 2012) from magnetic resonance images obtained at four different scanners, and are shown in Figure 4 (left). In total, we had 4196 scans of 1886 participants aged between 4 and 93 years, with between 1 and 7 scans per participant. Our interest concerned how the lifespan trajectory of hippocampal volume depends on socioeconomic status. For participants below the age of twenty, we defined socioeconomic status based on their father’s and mother’s years of completed education and income, and above the age of twenty we defined it based on the participants’ own education and income. As these variables were typically only measured at a single timepoint, they were considered time-independent. Of the 1886 participants with hippocampal volume measurements, either their own or at least one parent’s education level was available from 1681 participants, while the corresponding number for income was 538. All timepoints for the 205 participants with no measurement of socioeconomic status were also included in the analyses, yielding a total of 7130 level-1 units.

Since all outcomes were continuous, we used a unit link function and measurement model

$$y_i = \mathbf{d}'_{s,i} \boldsymbol{\beta}_s + d_{h,i} \{ \mathbf{x}'_{h,i} \boldsymbol{\beta}_h + f(a_i) \} + \eta_1^{(2)} \mathbf{z}'_i \boldsymbol{\lambda}_1 + d_{h,i} \eta_2^{(2)} + \epsilon_i, \quad (23)$$

where  $\boldsymbol{\beta}_s$  contained the intercepts for the items measuring socioeconomic status and  $\mathbf{d}_{s,i}$  was a vector whose  $k$ th element was an indicator for the event that the  $i$ th level-1 unit measured the  $k$ th socioeconomic status item. Variable  $d_{h,i} \in \{0, 1\}$  indicated the event that the  $i$ th level-1 unit was a measurement of hippocampal volume,  $\mathbf{x}_{h,i}$  was a vector of linear regression terms for scanner, sex, and intracranial volume, and  $\boldsymbol{\beta}_h$  were corresponding regression

coefficients. The age of the participant to which the  $i$ th level-1 unit belonged was denoted  $a_i$ , and  $f(\cdot)$  was a smooth function composed as a linear combination of fifteen cubic regression splines according to (5). Latent socioeconomic status was represented by  $\eta_1^{(2)}$ , and  $\boldsymbol{\lambda}_1 = (\lambda_1, \dots, \lambda_8)'$  was a vector of factor loadings. Factor loadings for paternal, maternal, and the participant's own education level were represented by  $\lambda_1, \dots, \lambda_3$ , and the corresponding factor loadings for paternal, maternal, and the participant's own income were represented by  $\lambda_4, \dots, \lambda_6$ . Accordingly, when the  $i$ th level-1 unit was a measurement of income or education,  $\mathbf{z}_i$  was an indicator vector which ensured that the correct factor loading among  $\lambda_1, \dots, \lambda_6$  was multiplied by  $\eta_1^{(2)}$ . Finally,  $\lambda_7$  represented the effect of latent socioeconomic status on hippocampal volume, and  $\lambda_8$  the interaction effect of age and socioeconomic status on hippocampal volume. Hence, when the  $i$ th level-1 unit was a measurement of hippocampal volume,  $\mathbf{z}'_i = (0, \dots, 0, 1, a_i)$ . Since the data contained repeated scans, a random intercept for hippocampal volume  $\eta_2^{(2)}$  was also included. A heteroscedastic model for the residuals was assumed,  $\epsilon_i \sim N(0, \sigma_{g(i)}^2)$ , where  $g(i) = 1$  if the  $i$ th level-1 unit was a measurement of income,  $g(i) = 2$  if it was a measurement of education level, and  $g(i) = 3$  if it was a measurement of hippocampal volume. The structural model was simply  $\boldsymbol{\eta}^{(2)} = \boldsymbol{\zeta}^{(2)} \sim N(\mathbf{0}, \boldsymbol{\Psi}^{(2)})$  where  $\boldsymbol{\Psi}^{(2)} = \text{diag}(\psi_1^{(2)}, \psi_2^{(2)})$ . Assuming zero correlation between level-2 disturbances was required for identifiability, since  $\eta_2^{(2)}$  depended on  $\eta_1^{(2)}$  through  $\lambda_7$  and  $\lambda_8$ .

The model was estimated with the profile likelihood method of Section 2.3, using the `gamm()` function from 'mgcv' (Wood 2017) in step (13), as it allows heteroscedastic residuals. Income and education variables were log-transformed to obtain response values closer to a normal distribution. When fitting the models, all quantitative variables were transformed to have zero mean and unit standard deviations. For identifiability,  $\lambda_1$  was fixed to unity on the transformed scale used in model fitting. The model described above had seven free factor loadings,  $\lambda_2, \dots, \lambda_8$ , and we compared it to constrained versions using the marginal Akaike information criterion (see Section 2.1 of Supplement C for details). The chosen model had all education loadings and all income loadings set equal, i.e.,  $\lambda_1 = \lambda_2 = \lambda_3$  and  $\lambda_4 = \lambda_5 = \lambda_6$ .

Table 2 shows the estimated parametric effects of main interest. Item intercepts  $\beta_s$  are shown in Table 2 of Supplement C. Standard errors are not reported for variance components, as their likelihood is typically not regular. We note that naive standard errors were very close to the asymptotic standard errors for all parameters, and as expected, higher total intracranial volume and being male were associated with higher hippocampal volume. From the estimated standard deviation of the random intercept for hippocampal volume and the residual standard deviation for hippocampal volume, we found an intraclass correlation (ICC) of  $= 600^2 / (600^2 + 133^2) = 0.95$ . An ICC this high implies that the variation between individuals was much larger than the variation between different timepoints of the same individual, as is also clear from the raw data plot in Figure 4 (left). The estimated factor loading for income was positive, with 95% confidence interval [0.16, 0.37], indicating that both education and income were positively related to the latent construct  $\eta_1^{(2)}$ . It also follows that the difference between mean socioeconomic status and a socioeconomic status one standard deviation above the mean was associated with a difference in education level of  $\exp(\hat{\beta}_{s3} + \hat{\lambda}_3 \sqrt{\hat{\psi}_1^{(2)}}) - \exp(\hat{\beta}_{s3}) = 2$  years and with difference in annual income of  $\exp(\hat{\beta}_{s6} + \hat{\lambda}_6 \sqrt{\hat{\psi}_1^{(2)}}) - \exp(\hat{\beta}_{s6}) = 95 \times 10^3$  NOK, where we have taken  $\hat{\beta}_{s3} = 2.81$  and



Table 2: Parametric terms in model of hippocampal volume and socioeconomic status.

Parameter	Estimate	SE	SE-naive	Units
<i>Effects on hippocampal volume</i>				
Scanner ousAvanto, $\beta_{h1}$	-76.9	57.5	57.5	mm <sup>3</sup>
Scanner ousPrisma, $\beta_{h2}$	76.1	65.2	65.2	mm <sup>3</sup>
Scanner ousSkyra, $\beta_{h3}$	240	58.5	58.4	mm <sup>3</sup>
Total intracranial volume, $\beta_{h4}$	0.00199	9.09E-05	9.09E-05	mm <sup>3</sup> /mm <sup>3</sup>
Sex=Male, $\beta_{h5}$	220	33.1	33.1	mm <sup>3</sup>
<i>Factor loadings</i>				
Education, $\lambda_1 = \lambda_2 = \lambda_3$	0.169	-	-	log(years)
Income, $\lambda_4 = \lambda_5 = \lambda_6$	0.265	0.0523	-	log(NOK)
Hippocampus, $\lambda_7$	58.2	32.4	-	mm <sup>3</sup>
<i>Variance components</i>				
Socioeconomic status, $\sqrt{\psi_1^{(2)}}$	0.67	-	-	-
Hippocampus, $\sqrt{\psi_2^{(2)}}$	600	-	-	mm <sup>3</sup>
Income residual, $\sigma_1$	0.595	-	-	log(NOK)
Education residual, $\sigma_2$	0.125	-	-	log(years)
Hippocampus residual, $\sigma_3$	133	-	-	mm <sup>3</sup>

NOK denotes Norwegian kroner, with 10 NOK $\approx$ 1 EUR. Scanner effects are relative to 'ntnuSkyra', see Figure 4 (left). Units mm<sup>3</sup>/mm<sup>3</sup> for total intracranial volume represent mm<sup>3</sup> of hippocampus per mm<sup>3</sup> of total intracranial volume.

$\hat{\beta}_{s6} = 13.1$  from Table 2 of Supplement C. Note that this effect is not additive on the natural scale, since education and income levels were log-transformed.

Figure 4 (right) shows the estimated hippocampal trajectories at three levels of socioeconomic status. From Table 2, the estimated main effect of socioeconomic status on hippocampal volume,  $\hat{\lambda}_7$  had 95% confidence interval containing zero,  $[-5.3, 121.7]$  mm<sup>3</sup>, and was hence not significant at a 5% level. From the point estimate, we see that a one standard deviation increase in socioeconomic status was associated with an increase in hippocampal volume of  $\hat{\lambda}_7\sqrt{\hat{\psi}_1^{(2)}} = 39$  mm<sup>3</sup>. For comparison, the rate of increase seen during childhood in Figure 4 (left) was around 50 mm<sup>3</sup>/year, the rate of decline during adulthood around 10-15 mm<sup>3</sup>/year, increasing to 90-100 mm<sup>3</sup>/year in old age. Assuming no birth cohort effects and representative sampling, the presence of a constant effect  $\lambda_7$  and the absence of an interaction effect  $\lambda_8$ , would imply that socioeconomic status affects early life brain development, rather than the rate of change at any point later in life. However, this analysis is inconclusive with regards to such a conclusion.

## 4 Discussion

We have presented the GALAMM framework for multilevel latent variable modeling, which combines structural equation and item response models' ability to accurately model a measurement process with generalized additive models' ability to flexibly estimate smooth functional relationships. Simulation experiments reported in Supplements B suggest that

the algorithm has low bias even with moderate sample sizes, and that confidence intervals derived from the asymptotic standard error formulas in Section 2.4 have close to nominal coverage.

A number of extensions to the application examples shown in Section 3 are possible. In Section 3.1, we assumed measurement invariance across age, which could be relaxed with age-dependent factor loadings, yielding a non-uniform differential item functioning model (Swaminathan & Rogers 1990). In the factor-by-curve model in Section 3.2, random slopes of age could be included at level 3, allowing estimation of how individual change is correlated across cognitive domains as well as level-slope correlation within domains. These topics were studied in a recent meta analysis (Tucker-Drob et al. 2019) in which all the contributing studies had analyzed samples of adults using linear models. GALAMM would more easily allow such studies of coupled cognitive change across the lifespan, since the nonlinear effect of age is flexibly handled by smooth terms. An extension of the latent covariates model in Section 3.3 would be to estimate the effect of socioeconomic status on a larger number of brain regions. Smoothing parameters could be shared as in Section 3.2, and the impact of socioeconomic status investigated for each brain region.

The GALAMM framework naturally accommodates models with responses of different type, by letting the link function in the response distribution (3) vary with level-1 unit  $i$ . An alternative approach to handling multiple response types is offered by latent response models (Muthén 1984), in which constrained responses are assumed to be thresholded realizations of a continuous latent response, can also be accommodated within the framework. If such data were available, this would allow including, e.g., ordinal and categorical variables in the measurement model for socioeconomic status in Section 3.3.

An alternative to the proposed profile likelihood algorithm is to directly maximize the log-likelihood of the nonlinear mixed model in the reduced form (11). The main computational hurdle is to evaluate the likelihood function, which requires integrating over all latent variables. As GALAMMs with smooth terms always have one more hierarchical level than a corresponding GLLAMM, these integrals become high-dimensional. Rabe-Hesketh et al. (2005) developed an adaptive Gauss-Hermite quadrature algorithm for numerical integration, which can be combined with quasi-Newton methods like L-BFGS-B. Unfortunately, the algorithm is not currently available in R, but we will address this in future work.

## SUPPLEMENTARY MATERIAL

**Supplement A: Mixed Model Representation** Derivation of mixed model representation of GALAMM. (pdf document)

**Supplement B: Simulation Experiments** Results from simulation experiments. (pdf document)

**Supplement C: Case Studies** Additional results for case studies. (pdf document)

**galamm-scripts** R scripts required to run all analyses and simulations. (zip file)

## References

- Arminger, G. & Muthén, B. O. (1998), ‘A Bayesian approach to nonlinear latent variable models using the Gibbs sampler and the Metropolis-Hastings algorithm’, *Psychometrika* **63**(3), 271–300.
- Bates, D., Mächler, M., Bolker, B. & Walker, S. (2015), ‘Fitting Linear Mixed-Effects Models Using lme4’, *Journal of Statistical Software* **67**(1), 1–48.
- Blackburn, H. L. & Benton, A. L. (1959), ‘Revised administration and scoring of the Digit Span Test.’, *Journal of Consulting Psychology* **21**(2), 139.
- Breslow, N. E. & Clayton, D. G. (1993), ‘Approximate Inference in Generalized Linear Mixed Models’, *Journal of the American Statistical Association* **88**(421), 9–25.
- Byrd, R. H., Lu, P., Nocedal, J. & Zhu, C. (1995), ‘A Limited Memory Algorithm for Bound Constrained Optimization’, *SIAM Journal on Scientific Computing* **16**(5), 1190–1208.
- Coull, B. A., Ruppert, D. & Wand, M. P. (2001), ‘Simple Incorporation of Interactions into Additive Models’, *Biometrics* **57**(2), 539–545.
- Delis, D. C., Kramer, J. H., Kaplan, E. & Ober, B. A. (2000), *CVLT, California Verbal Learning Test: Second Edition*, Psychological Corporation, San Antonio, TX.
- Dubois, B., Hampel, H., Feldman, H. H., Scheltens, P., Aisen, P., Andrieu, S., Bakardjian, H., Benali, H., Bertram, L., Blennow, K., Broich, K., Cavedo, E., Crutch, S., Dartigues, J.-F., Duyckaerts, C., Epelbaum, S., Frisoni, G. B., Gauthier, S., Genthon, R., Gouw, A. A., Habert, M.-O., Holtzman, D. M., Kivipelto, M., Lista, S., Molinuevo, J.-L., O’Byrant, S. E., Rabinovici, G. D., Rowe, C., Salloway, S., Schneider, L. S., Sperling, R., Teichmann, M., Carrillo, M. C., Cummings, J., Jack Jr, C. R. & Proceedings of the Meeting of the International Working Group (IWG) and the American Alzheimer’s Association on “The Preclinical State of AD”; July 23, USA, . W. D. (2016), ‘Preclinical Alzheimer’s disease: Definition, natural history, and diagnostic criteria’, *Alzheimer’s & Dementia* **12**(3), 292–323.
- Fahrmeir, L. & Raach, A. (2007), ‘A Bayesian Semiparametric Latent Variable Model for Mixed Responses’, *Psychometrika* **72**(3), 327.
- Fischl, B. (2012), ‘FreeSurfer’, *NeuroImage* **62**(2), 774–781.
- Fjell, A. M., Idland, A.-V., Sala-Llonch, R., Watne, L. O., Borza, T., Brækhus, A., Lona, T., Zetterberg, H., Blennow, K., Wyller, T. B. & Walhovd, K. B. (2018), ‘Neuroinflammation and Tau Interact with Amyloid in Predicting Sleep Problems in Aging Independently of Atrophy’, *Cerebral Cortex* **28**(8), 2775–2785.
- Gilbert, P. & Varadhan, R. (2019), *numDeriv: Accurate Numerical Derivatives*. R package version 2016.8-1.1.
- Hastie, T. & Tibshirani, R. (1993), ‘Varying-Coefficient Models’, *Journal of the Royal Statistical Society: Series B (Methodological)* **55**(4), 757–779.

- Jeon, M. & Rabe-Hesketh, S. (2012), ‘Profile-Likelihood Approach for Estimating Generalized Linear Mixed Models With Factor Structures’, *Journal of Educational and Behavioral Statistics* **37**(4), 518–542.
- Lee, S.-Y. & Zhu, H.-T. (2000), ‘Statistical analysis of nonlinear structural equation models with continuous and polytomous data’, *British Journal of Mathematical and Statistical Psychology* **53**(2), 209–232.
- Livingston, G., Sommerlad, A., Orgeta, V., Costafreda, S. G., Huntley, J., Ames, D., Ballard, C., Banerjee, S., Burns, A., Cohen-Mansfield, J., Cooper, C., Fox, N., Gitlin, L. N., Howard, R., Kales, H. C., Larson, E. B., Ritchie, K., Rockwood, K., Sampson, E. L., Samus, Q., Schneider, L. S., Selbæk, G., Teri, L. & Mukadam, N. (2017), ‘Dementia prevention, intervention, and care’, *The Lancet* **390**(10113), 2673–2734.
- Marra, G. & Wood, S. N. (2012), ‘Coverage Properties of Confidence Intervals for Generalized Additive Model Components’, *Scandinavian Journal of Statistics* **39**(1), 53–74.
- McArdle, J. J., Ferrer-Caja, E., Hamagami, F. & Woodcock, R. W. (2002), ‘Comparative longitudinal structural analyses of the growth and decline of multiple intellectual abilities over the life span’, *Developmental Psychology* **38**(1), 115–142.
- Mehta, P. D. & Neale, M. C. (2005), ‘People are variables too: Multilevel structural equations modeling’, *Psychological Methods* **10**(3), 259–284.
- Meredith, W. & Tisak, J. (1990), ‘Latent curve analysis’, *Psychometrika* **55**(1), 107–122.
- Muthén, B. (1984), ‘A general structural equation model with dichotomous, ordered categorical, and continuous latent variable indicators’, *Psychometrika* **49**(1), 115–132.
- Muthén, B. O. (2002), ‘Beyond SEM: General Latent Variable Modeling’, *Behaviormetrika* **29**(1), 81–117.
- Nelder, J. A. & Mead, R. (1965), ‘A Simplex Method for Function Minimization’, *The Computer Journal* **7**(4), 308–313.
- Nilsson, L.-G., Sternäng, O., Rönnlund, M. & Nyberg, L. (2009), ‘Challenging the notion of an early-onset of cognitive decline’, *Neurobiology of Aging* **30**(4), 521–524.
- Noble, K. G., Houston, S. M., Kan, E. & Sowell, E. R. (2012), ‘Neural correlates of socioeconomic status in the developing human brain’, *Developmental Science* **15**(4), 516–527.
- Novick, M. R. (1966), ‘The axioms and principal results of classical test theory’, *Journal of Mathematical Psychology* **3**(1), 1–18.
- Nyberg, L., Magnussen, F., Lundquist, A., Baaré, W., Bartrés-Faz, D., Bertram, L., Boraxbekk, C. J., Brandmaier, A. M., Drevon, C. A., Ebmeier, K., Ghisletta, P., Henson, R. N., Junqué, C., Kievit, R., Kleemeyer, M., Knights, E., Kühn, S., Lindenberger, U., Penninx, B. W. J. H., Pudas, S., Sørensen, Ø., Vaqué-Alcázar, L., Walhovd, K. B. & Fjell, A. M. (2021), ‘Educational attainment does not influence brain aging’, *Proceedings of the National Academy of Sciences* **118**(18).

- Oud, J. H. L. & Jansen, R. A. R. G. (2000), ‘Continuous time state space modeling of panel data by means of SEM’, *Psychometrika* **65**(2), 199–215.
- Parke, W. R. (1986), ‘Pseudo Maximum Likelihood Estimation: The Asymptotic Distribution’, *The Annals of Statistics* **14**(1), 355–357.
- Pinheiro, J., Bates, D., DebRoy, S., Sarkar, D. & R Core Team (2020), *nlme: Linear and Nonlinear Mixed Effects Models*. R package version 3.1-150.
- Proust-Lima, C., Amieva, H. & Jacqmin-Gadda, H. (2013), ‘Analysis of multivariate mixed longitudinal data: A flexible latent process approach’, *British Journal of Mathematical and Statistical Psychology* **66**(3), 470–487.
- Rabe-Hesketh, S., Skrondal, A. & Pickles, A. (2004), ‘Generalized multilevel structural equation modeling’, *Psychometrika* **69**(2), 167–190.
- Rabe-Hesketh, S., Skrondal, A. & Pickles, A. (2005), ‘Maximum likelihood estimation of limited and discrete dependent variable models with nested random effects’, *Journal of Econometrics* **128**(2), 301–323.
- Raz, N. & Lindenberger, U. (2011), ‘Only time will tell: Cross-sectional studies offer no solution to the age–brain–cognition triangle: Comment on Salthouse (2011).’, *Psychological Bulletin* **137**(5), 790–795.
- Rönnlund, M., Nyberg, L., Bäckman, L. & Nilsson, L.-G. (2005), ‘Stability, growth, and decline in adult life span development of declarative memory: Cross-sectional and longitudinal data from a population-based study.’, *Psychology and Aging* **20**(1), 3–18.
- Ruppert, D., Wand, M. P. & Carroll, R. J. (2003), *Semiparametric Regression*, Cambridge University Press, Cambridge, U.K.
- Salthouse, T. A. (2009), ‘When does age-related cognitive decline begin?’, *Neurobiology of Aging* **30**(4), 507–514.
- Schaie, K. W. (2009), “‘When does age-related cognitive decline begin?’” Salthouse again reifies the “cross-sectional fallacy”, *Neurobiology of Aging* **30**(4), 528–529.
- Schall, R. (1991), ‘Estimation in Generalized Linear Models with Random Effects’, *Biometrika* **78**(4), 719–727.
- Skrondal, A. & Rabe-Hesketh, S. (2004), *Generalized Latent Variable Modeling*, Interdisciplinary Statistics Series, Chapman and Hall/CRC, Boca Raton, Florida.
- Song, X.-Y., Lu, Z.-H., Cai, J.-H. & Ip, E. H.-S. (2013), ‘A Bayesian Modeling Approach for Generalized Semiparametric Structural Equation Models’, *Psychometrika* **78**(4), 624–647.
- Sørensen, Ø., Walhovd, K. B. & Fjell, A. M. (2021), ‘A recipe for accurate estimation of lifespan brain trajectories, distinguishing longitudinal and cohort effects’, *NeuroImage* **226**, 117596.

- Spearman, C. (1904), ‘“General Intelligence,” Objectively Determined and Measured’, *The American Journal of Psychology* **15**(2), 201–292.
- Staff, R. T., Murray, A. D., Ahearn, T. S., Mustafa, N., Fox, H. C. & Whalley, L. J. (2012), ‘Childhood socioeconomic status and adult brain size: Childhood socioeconomic status influences adult hippocampal size’, *Annals of Neurology* **71**(5), 653–660.
- Swaminathan, H. & Rogers, H. J. (1990), ‘Detecting Differential Item Functioning Using Logistic Regression Procedures’, *Journal of Educational Measurement* **27**(4), 361–370.
- Tucker-Drob, E. M., Brandmaier, A. M. & Lindenberger, U. (2019), ‘Coupled cognitive changes in adulthood: A meta-analysis.’, *Psychological Bulletin* **145**(3), 273–301.
- Venables, W. N. & Ripley, B. D. (2002), *Modern Applied Statistics with S*, fourth edn, Springer, New York. ISBN 0-387-95457-0.
- Walhovd, K. B., Bråthen, A. C. S., Panizzon, M. S., Mowinckel, A. M., Sørensen, Ø., de Lange, A.-M. G., Krogsrud, S. K., Håberg, A., Franz, C. E., Kremen, W. S. & Fjell, A. M. (2020), ‘Within-session verbal learning slope is predictive of lifespan delayed recall, hippocampal volume, and memory training benefit, and is heritable’, *Scientific Reports* **10**(1), 21158.
- Walhovd, K. B., Krogsrud, S. K., Amlien, I. K., Bartsch, H., Bjørnerud, A., Due-Tønnessen, P., Grydeland, H., Hagler, D. J., Håberg, A. K., Kremen, W. S., Ferschmann, L., Nyberg, L., Panizzon, M. S., Rohani, D. A., Skranes, J., Storsve, A. B., Sølsnes, A. E., Tamnes, C. K., Thompson, W. K., Reuter, C., Dale, A. M. & Fjell, A. M. (2016), ‘Neurodevelopmental origins of lifespan changes in brain and cognition’, *Proceedings of the National Academy of Sciences* **113**(33), 9357–9362.
- Wood, S. (2017), *Generalized Additive Models: An Introduction with R*, second edn, Chapman and Hall/CRC.
- Wood, S. N. (2003), ‘Thin Plate Regression Splines’, *Journal of the Royal Statistical Society. Series B (Statistical Methodology)* **65**(1), 95–114.
- Wood, S. N., Scheipl, F. & Faraway, J. J. (2013), ‘Straightforward intermediate rank tensor product smoothing in mixed models’, *Statistics and Computing* **23**(3), 341–360.
- Wood, S. & Scheipl, F. (2020), *gamm4: Generalized Additive Mixed Models Using 'mgcv' and 'lme4'*. R package version 0.2-6.
- Woods, S. P., Delis, D. C., Scott, J. C., Kramer, J. H. & Holdnack, J. A. (2006), ‘The California Verbal Learning Test – second edition: Test-retest reliability, practice effects, and reliable change indices for the standard and alternate forms’, *Archives of Clinical Neuropsychology* **21**(5), 413–420.

# Supplement B: Simulation Experiments

This supplementary document describes simulation experiments closely mimicking the case studies presented in Sections 3.1, 3.2, and 3.3 of the main manuscript. All analyses were done in R 4.0.0 (R Core Team 2020). In addition to the packages cited in the text, 'furr' (Vaughan & Dancho 2021) and 'future' (Bengtsson 2021) were used for parallel computation, 'moments' (Komsta & Novomestky 2015) and 'mvtnorm' (Genz et al. 2020) for multivariate analysis and random number generation, and 'dplyr' (Wickham et al. 2021), 'stringr' (Wickham 2019), and 'tidyr' (Wickham 2020) for data preparation. All plots were produced with 'ggplot2' (Wickham 2016) with additional functionality from 'gghalves' (Tiedemann 2020), 'ggthemes' (Arnold 2021), 'latex2exp' (Meschiari 2021), 'patchwork' (Pedersen 2020), and 'scales' (Wickham & Seidel 2020).

## 1 Simulations with Latent Response Models

Simulation experiments were conducted based on the model estimated in Section 3.1 of the main manuscript. The Laplace approximation used to fit the GAMM in equation 13 of the main manuscript is asymptotically consistent when both the number of participants and the number of observations per participant goes to infinity (Vonesh 1996), as is the overall profile likelihood algorithm (Parke 1986), but it is of interest to investigate their finite sample properties. To this end, we simulated 500 random datasets with 200, 500, and 1000 participants each. Probability distributions for age at measurement, time interval between measurements, and number of timepoints per participant were estimated from the LCBC data, and new values randomly sampled from these distributions. Since the participants are level-3 units, with an average number of timepoints equal to 1.88 and five

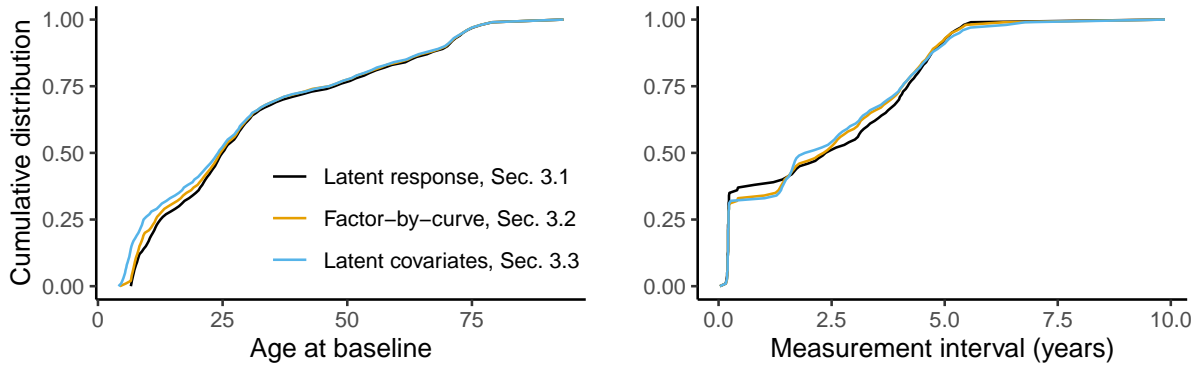


Figure 1: Cumulative distributions of baseline age and time interval between two consecutive measurements used in simulations experiments.

CVLT items observed at each timepoint, the expected total number of level-1 units with the three different samples sizes were 940, 4700, and 9400. The model set-up was identical to what is described in Section 3.1 of the main manuscript.

## 1.1 Description of Simulation Distributions

Each subject’s age at first timepoint was sampled from the cumulative distribution function shown in Figure 1 (left). The number of timepoints for each subject was multinomially distributed with probabilities shown in Figure 2. For subjects with more than one timepoint, the interval between two consecutive timepoints was distributed according to Figure 1 (right). For each subject, the age at each timepoint was computed as the sum of the baseline age and the cumulative sum of intervals between timepoints. The maximum age seen in the data was 93.4, and subject-timepoints with ages exceeding this value were removed, as the underlying smooth function for episodic memory was only defined up to the age of 93.4. In practice, this amounts to a very small number of subjects in each simulated sample.

Given a set of timepoints with corresponding ages for each participant, simulated re-



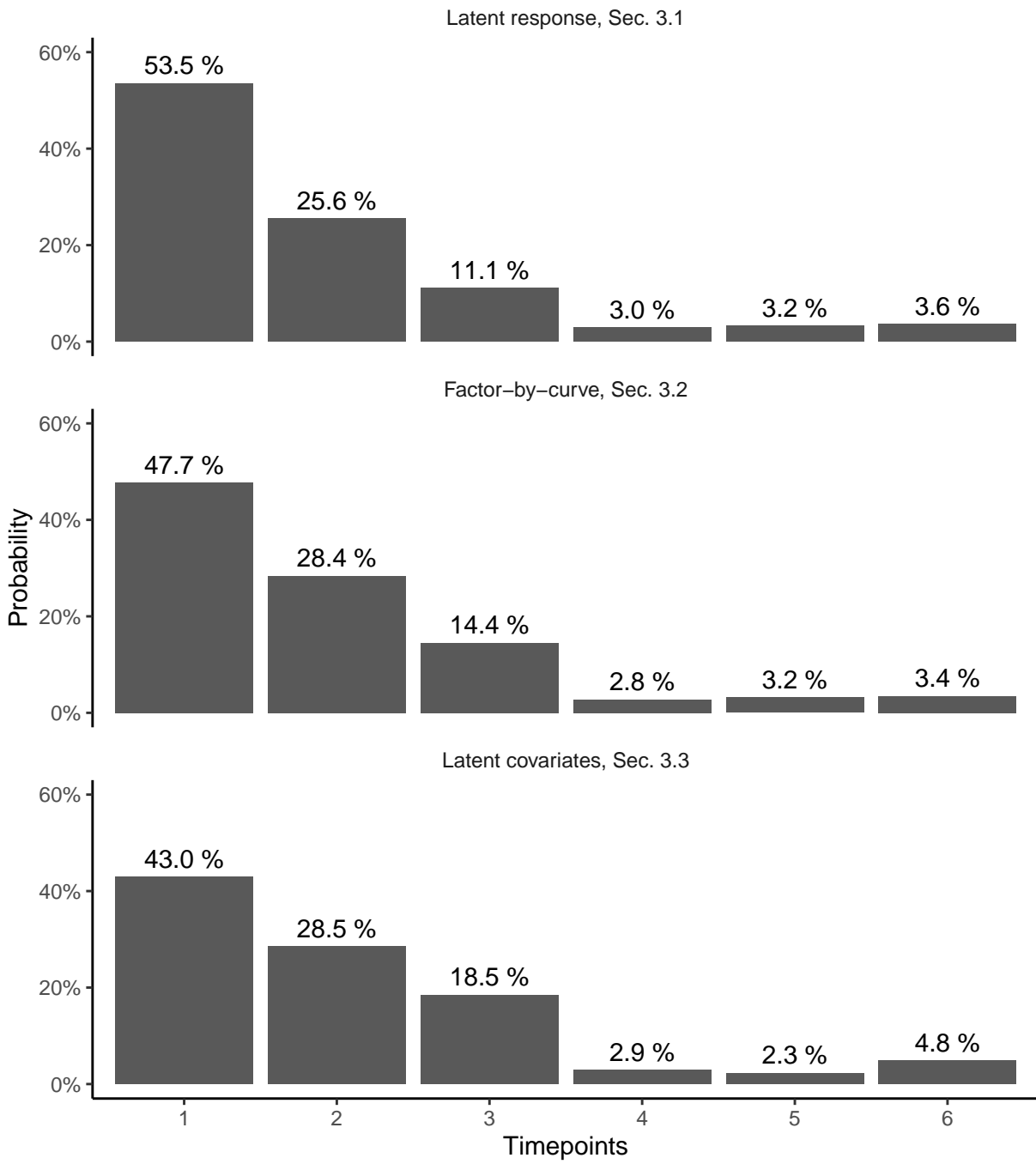


Figure 2: Probability of having number of timepoints between 1 and 6 in the simulation experiments.

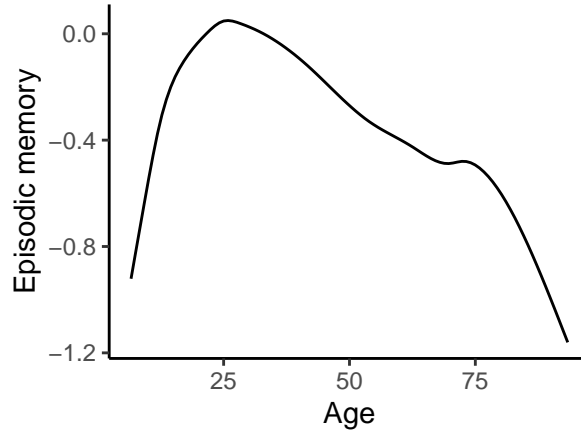


Figure 3: Lifespan trajectory for episodic memory used in simulation experiments with the latent response model.

sponses for each of the five CVLT items were generated according to a binomial model, with parameters exactly equal to the values estimated in the original analysis and shown in Section 3.1 of the main manuscript. This includes normally distributed latent variables  $\eta^{(2)}$  and  $\eta^{(3)}$ . The age trajectory  $h(w)$  used in the simulations was estimated from the fitted trajectory by linear interpolation, and is shown in Figure 3.

## 1.2 Simulation Results

Figure 4 shows simulation results for parametric terms, with relative bias between an estimate  $\hat{\beta}$  and the true value  $\beta$  defined as  $(\hat{\beta} - \beta)/\beta$ . Both the item effects and the retest effect showed a positive bias with 200 participants. For the item effects, this bias was considerably reduced with 500 participants, and close to zero with 1000 participants. For the retest effect, on the other hand, the bias was still around 2.5% with 1000 participants, down from around 6% with 200 participants. For the factor loadings, the bias was moderate at all sample sizes. Coverage of 95% confidence intervals for all parameter was close to nominal at all sample sizes. Confidence intervals for coverage probabilities here and in the

rest of the paper were computed using Wilson’s score interval with continuity correction as implemented in R’s `prop.test()` function (Newcombe 1998, Wilson 1927). Similar low bias was observed for estimated variance components (Figure 5). As shown in the third column of Figure 4, the mean square error (MSE) of all parameters decreased consistently with sample size. The ratio of MSE with 1000 participants to MSE with 200 participants ranged from 0.16 to 0.20, which is close to the expected value  $200/1000 = 0.20$  under root- $n$  consistency.

Figure 6 (left) shows that across-the-function coverage of pointwise confidence intervals are close to nominal for all sample sizes. The simultaneous confidence intervals had slightly below nominal coverage, around 93%. Hypothesizing that a larger basis would reduce bias with large sample sizes (e.g., Hall & Opsomer (2005)) and hence increase interval coverage, we performed an additional set of simulations using 30 cubic regression splines with 1000 participants. However, the results showed essentially no difference from using a basis of size 15. The center plot in Figure 6 shows that pointwise confidence intervals achieve close to nominal coverage by having above nominal coverage over parts of the range and below nominal coverage over other parts, as also demonstrated by Ruppert & Carroll (2000). Comparison with the true curve in Figure 3 suggests that the coverage is low in regions where the smooth curve changes rapidly, in childhood and in old age, and the coverage is high when the curve is close to linear, during most of adulthood. Squared bias and variance were computed separately at each age across Monte Carlo estimates, and then averaged across the full age range, and are shown in the right plot in Figure 6, together with their sum (MSE). Squared bias amounted to 20% of the MSE at 200 participants, 21.8% at 500 participants, and 18.6% at 1000 participants, suggesting that the proportion of bias is fairly constant within this range of sample sizes.

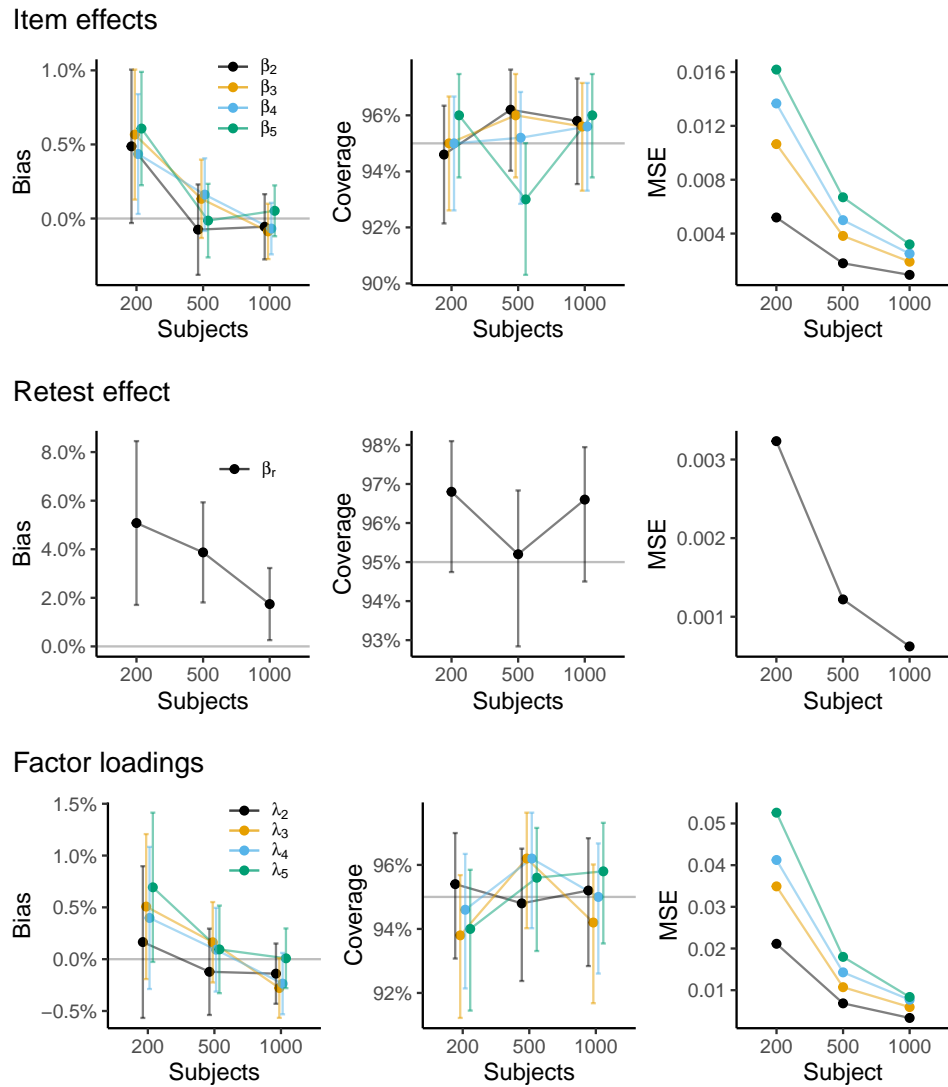


Figure 4: Simulation results for parametric terms. All points are averages over 500 Monte Carlo simulations, and error bars show 95% confidence intervals.

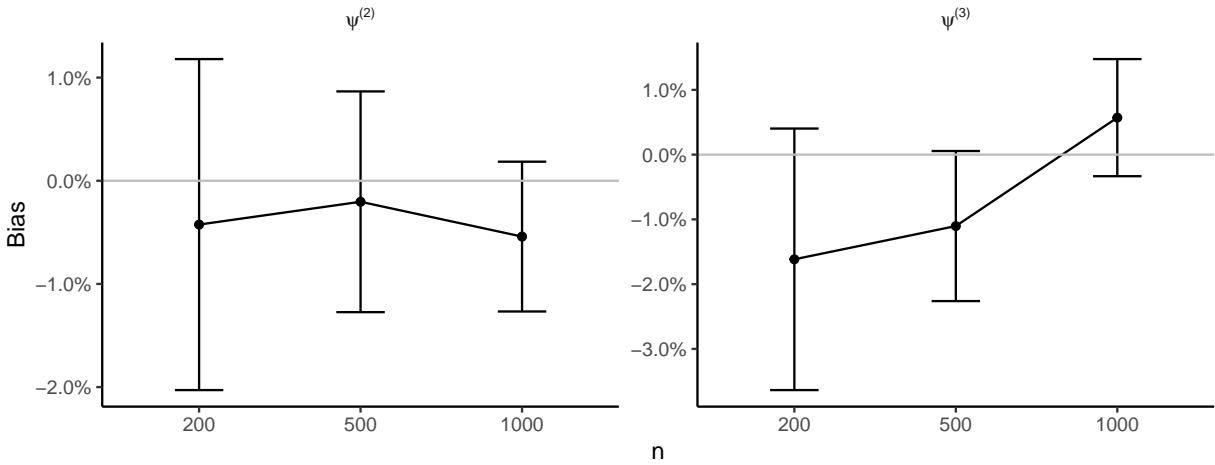


Figure 5: Mean bias in estimated variance components over 500 Monte Carlo simulations. Error bars represent 95% confidence intervals.

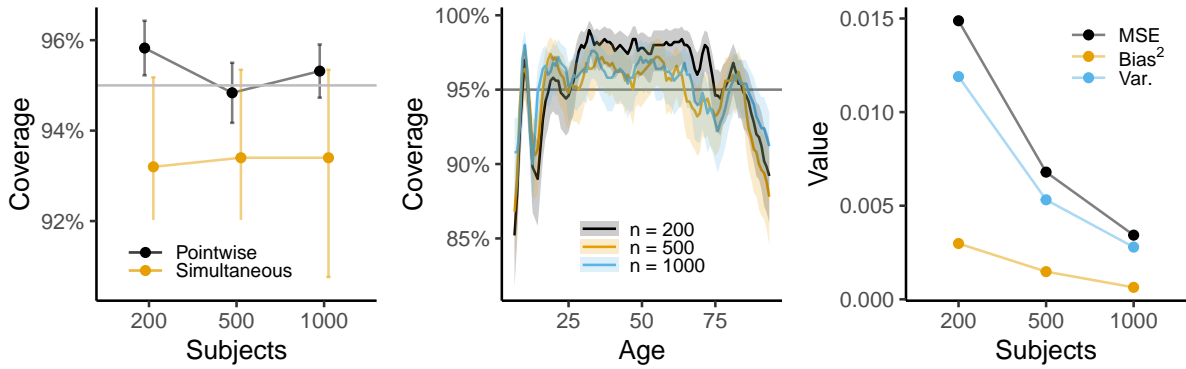


Figure 6: Simulation results for smooth terms. The left plot shows across-the-function coverage of pointwise confidence intervals and coverage of simultaneous confidence intervals. The center plot shows how coverage of pointwise intervals depends on age, and the right plot shows mean-square error, together with its bias-variance decomposition. Error bars and confidence bands represent 95% confidence intervals.

## 2 Simulations with Factor-by-Curves Interaction Models

Simulation experiments were performed with the goal of understanding the accuracy of the estimated correlations between latent variables at level 2 and level 3. Due to the high computational requirement, the factor loadings were fixed at their estimated values, such that only the GAMM part (eq. 13 in main manuscript) of the profile likelihood algorithm had to be computed. The simulated data were close to the real data and model estimates, but with level-2 correlation set to 0.5 rather than the estimated 1.0, and level-3 correlation set at the estimate 0.41. Hypothesizing that correlations would be more accurately estimated with an increasing number of timepoints per individuals, we considered (1) the original setting in which 45.9% of the participants were measured at a single timepoint, (2) a setting in which all participants had at least two timepoints, and (3) a setting in which all participants had at least three timepoints. These cases were combined with (a) a setting in which the particular tests taken at each timepoint followed the original data, and (b) a setting in which each participant had completed both the CVLT and the digit span test at each timepoint. For each setting, 100 Monte Carlo samples were generated.

### 2.1 Description of Simulation Distributions

The Monte Carlo simulations followed the steps described in Section 1.1. The empirical distributions of baseline age and time between measurements are shown in Figure 1 and the number of timepoints per individual are shown in Figure 2. In addition, Figure 7 shows the proportion of tests taken at each timepoint. In contrast to the other simulation experiments, in the factor-by-curve model the number of timepoints per individual and the

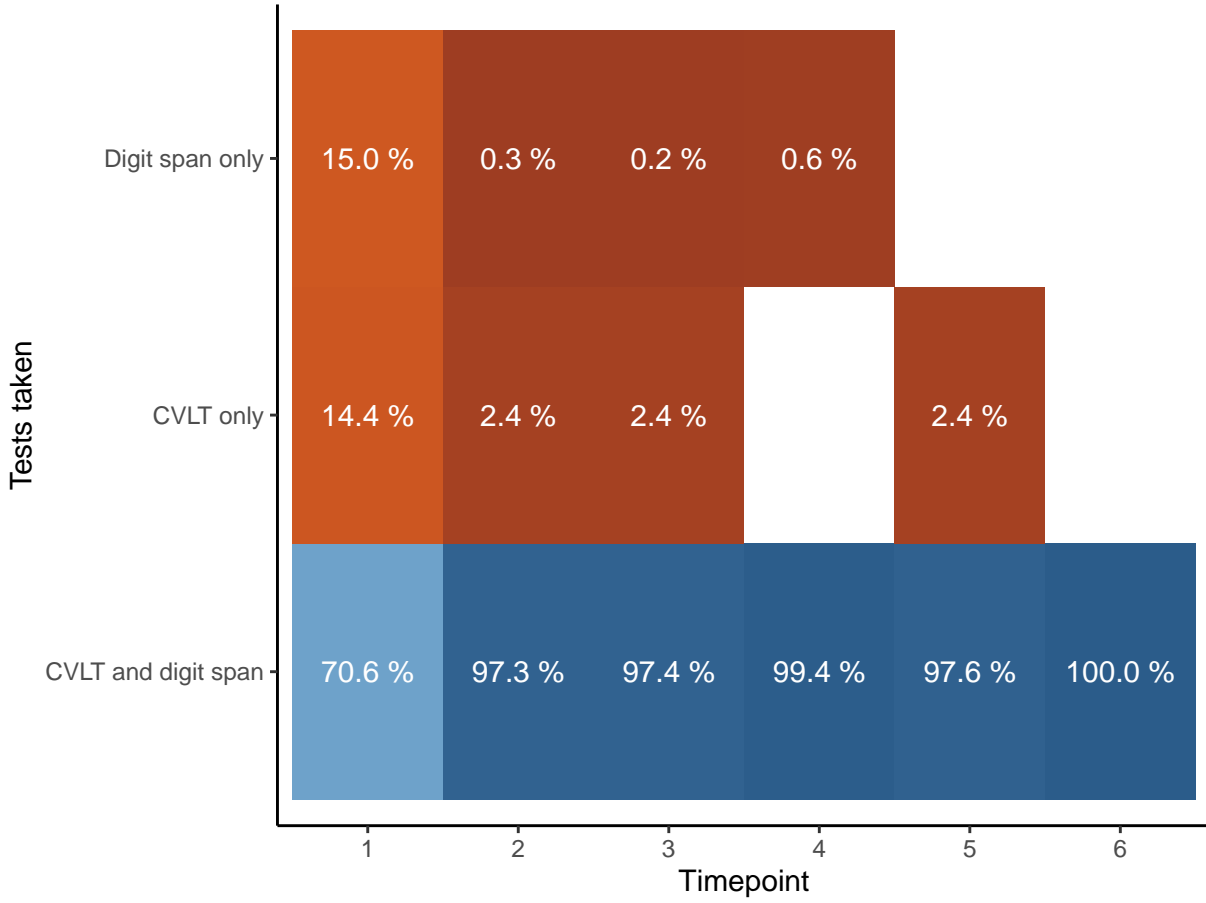


Figure 7: The plot shows, for each timepoint, the proportion of subjects which completed both tests or only one of the tests.

tests taken per timepoint were fixed at the values shown in Figures 2 and 7, rather than multinomially sampled with mean given by the values in the figures. However, the baseline age, time intervals, and the response, were randomly sampled.

The responses were directly sampled from the estimated model described in Section 3.2 of the main manuscript. The item intercepts were

$$\hat{\beta}_t = (-0.042, 0.49, 1.07, 1.44, 1.73, -0.53, 0.15)'$$

where the first five elements are CVLT items and the last two are digit span backward and digit span forward, respectively. The retest effects were  $\hat{\beta}_r = (0.14, 0.06)'$  for CVLT and

digit span, respectively, and the factor loadings were  $\hat{\boldsymbol{\lambda}}_1 = (1, 1.75, 2.34, 2.60, 2.79)'$  and  $\hat{\boldsymbol{\lambda}}_2 = (1, 0.95)'$ . The level-2 variances were  $\hat{\psi}_1^{(2)} = 0.065$  and  $\hat{\psi}_2^{(2)} = 0.001$ , and the level-2 correlation was fixed to 0.5, although it was estimated to 1 in the original analysis. The level-3 covariance matrix was

$$\hat{\boldsymbol{\Psi}}^{(3)} = \begin{pmatrix} 0.080 & 0.037 \\ 0.037 & 0.102 \end{pmatrix}.$$

## 2.2 Simulation Results

The results indicated that level-3 correlation was accurately estimated with minimal bias in all settings (Figure 8), whereas level-2 correlation was highly inaccurate. In the simulation setting closest to the original data (1a), the estimated level-2 correlation varied between -1 and +1, with a peak at 1 (Figure 9). Even with complete data and at least three timepoints per individual (3a), the distribution varied between 0 and 1, with a peak at 1. Importantly, this inaccurate estimation of level-2 correlation did not show negative consequences for the other model parameters. Across-the-function coverage of pointwise confidence intervals for smooth terms were close to nominal (Figure 10), and the root-mean-square error of the estimated smooth terms was not correlated with the estimated level-2 correlation (Figure 11).

## 3 Latent Covariates Model

Simulation experiments were performed based on the model estimated in Section 3.3 of the main manuscript. In particular, we were interested in understanding model selection with AIC as performed in Section 2.1 of Supplement C and the estimation of hippocampal volume trajectories as in Figure 4 of the main manuscript (right).



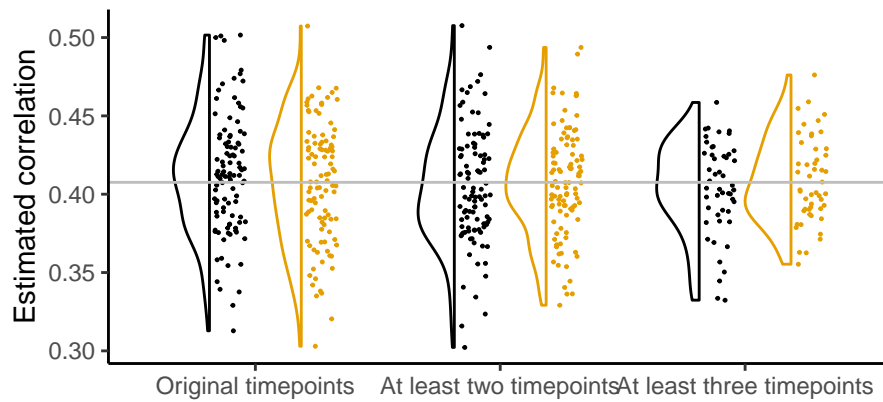


Figure 8: Distribution of estimated level-3 correlation across Monte Carlo samples. Horizontal gray line indicates the true correlation value.

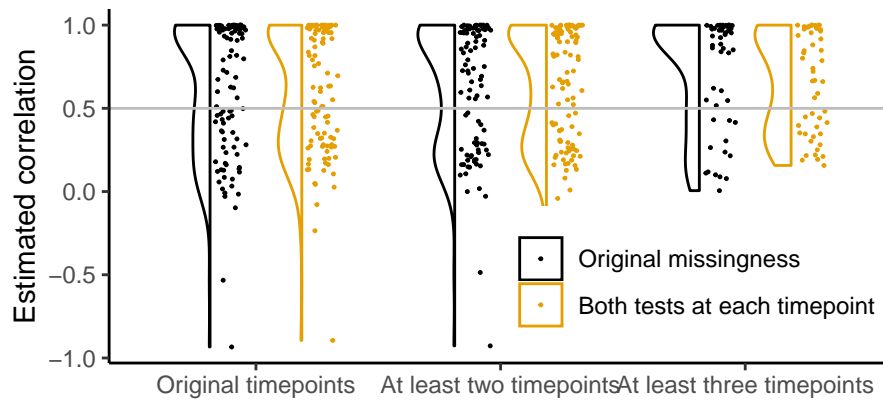


Figure 9: Distribution of estimated level-2 correlation across Monte Carlo samples. Horizontal gray line indicates the true correlation value.

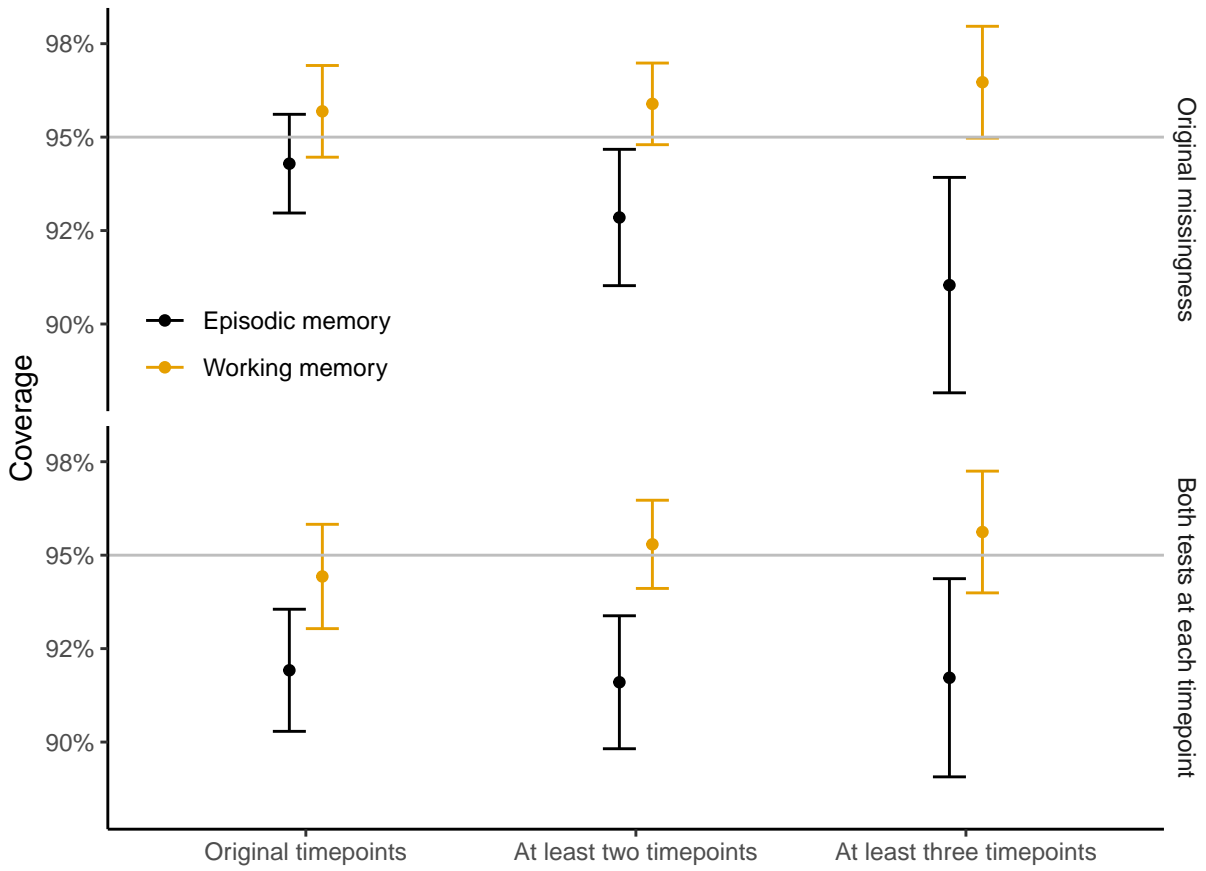


Figure 10: Across-the-function coverage of pointwise confidence intervals for smooth terms for episodic memory and working memory. Error bars show 95% confidence intervals.

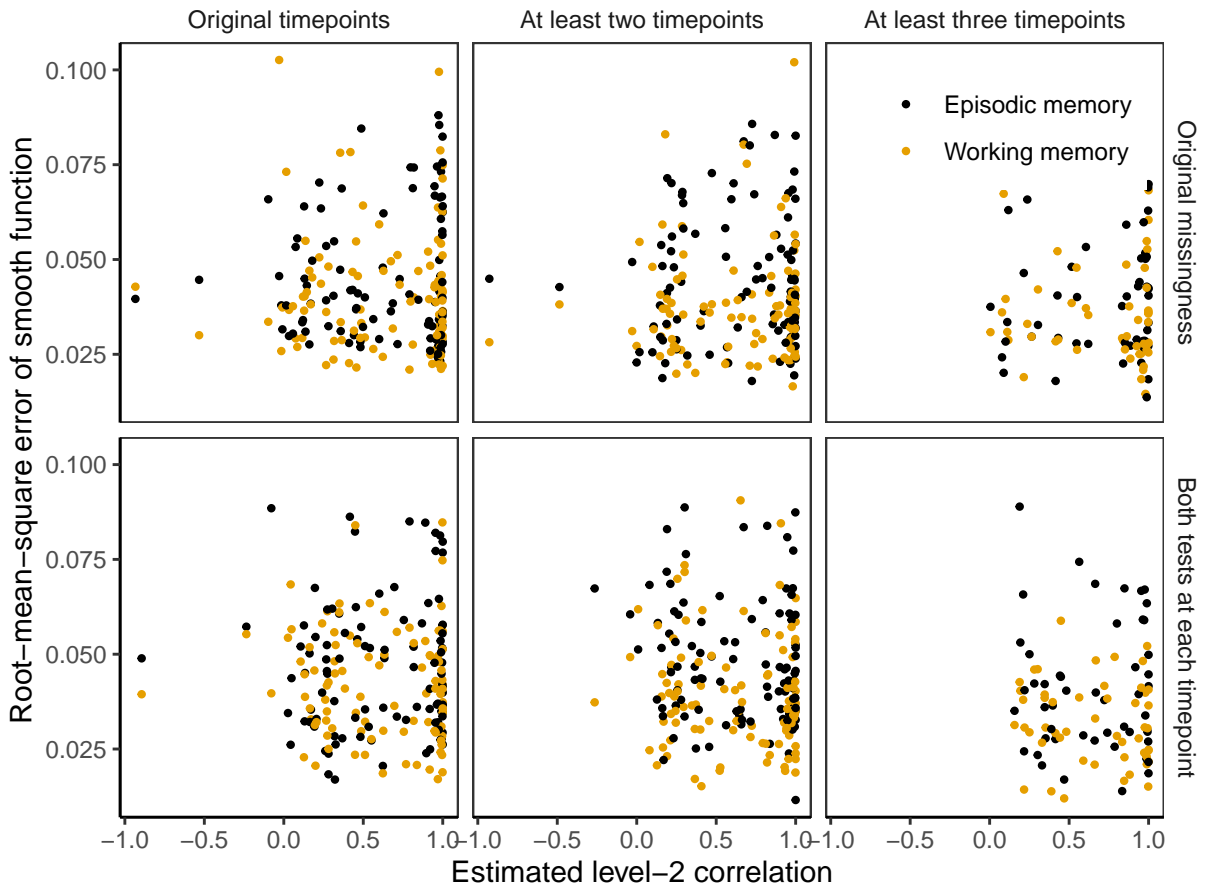


Figure 11: Scatter plot of root-mean-square error of estimated smooth functions and estimated level-2 correlation. The true level-2 correlation was 0.5.

### 3.1 Description of Simulation Distribution

We simulated data using estimated model parameters and a data structure closely following the real data, as shown in Figures 1 and 2. For simplicity, explanatory variables related to scanner, sex, and intracranial volume were not included in the simulations, but otherwise the model was identical to the one specified by equation 23 in the main manuscript, with parameter values reported in Table 2 of the main manuscript and Table 1 in Supplement C. The simulations were repeated with six discrete values of the interaction parameter  $\lambda_8$ , ranging from 0 to 0.12. Zero interaction implies that the trajectories for different levels of socioeconomic status are parallel, as in Figure 4 of the main manuscript (right), whereas a positive interaction implies that high socioeconomic status is associated with a slower rate of aging in adulthood. This is illustrated in Figure 12. For all parameter settings, 500 Monte Carlo samples with 1886 participants were randomly sampled, and models corresponding to (e) and (f) in Table 1 of Supplement C were fitted.

### 3.2 Simulation Results

Figure 13 (left) shows the performance of model selection with AIC and model selection with a one-sided hypothesis test at 5% significance level. That is, models (e) and (f) in Table 1 of Supplement C were compared. With true interaction zero, the probability of falsely rejecting the null hypothesis  $\lambda_8 = 0$  was around 5%, and the probability of AIC selecting the model containing this interaction term is close to the expected value of 16%. Furthermore, the curves suggest that we would have around 80% power to detect a moderate interaction  $\lambda_8 \approx 0.07$ . Figure 13 (right) shows the distribution of estimates  $\hat{\lambda}_8$  in the larger model (e) over all Monte Carlo samples. It is evident that the estimated interactions are symmetrically distributed around their true values. Also for the other factor loadings in

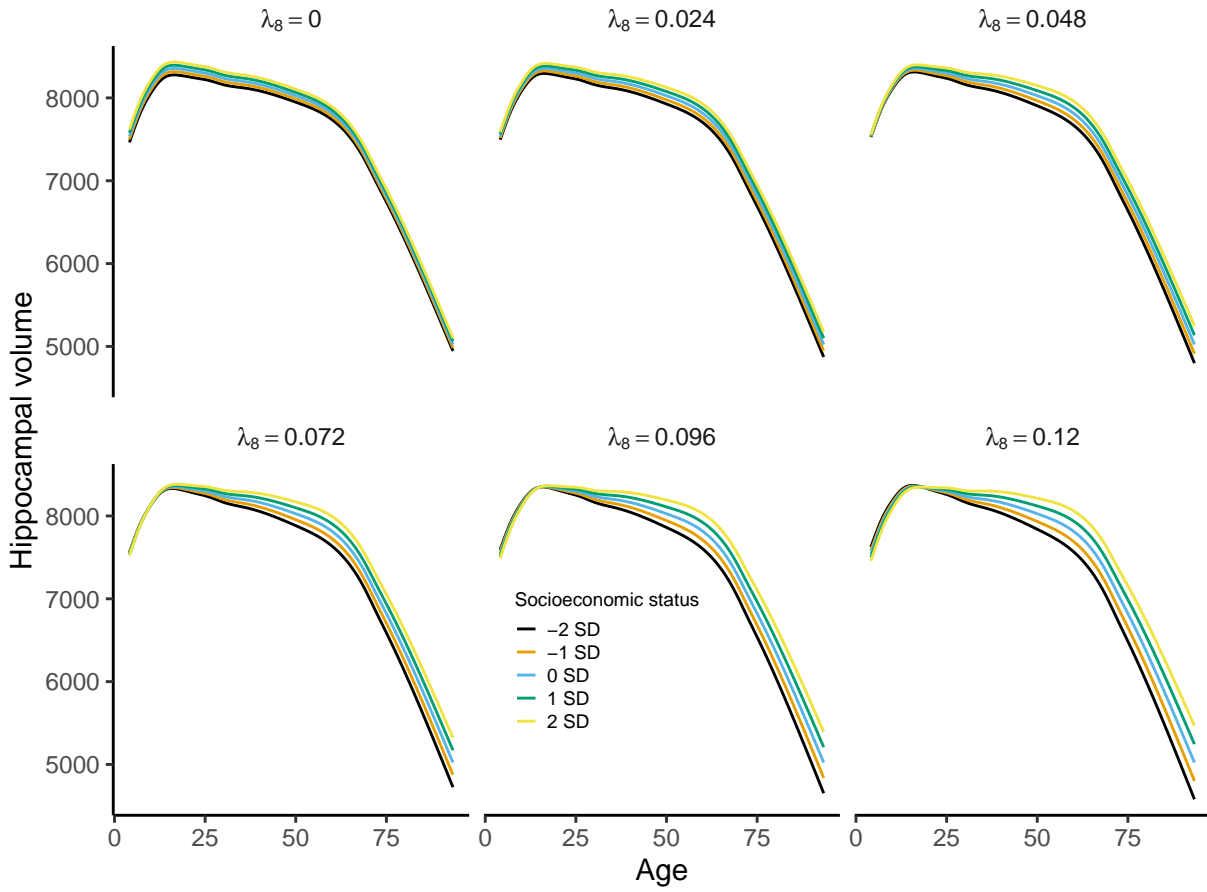


Figure 12: Visualization of the six interaction values  $\lambda_8$  used in simulation experiments with the latent covariates model.

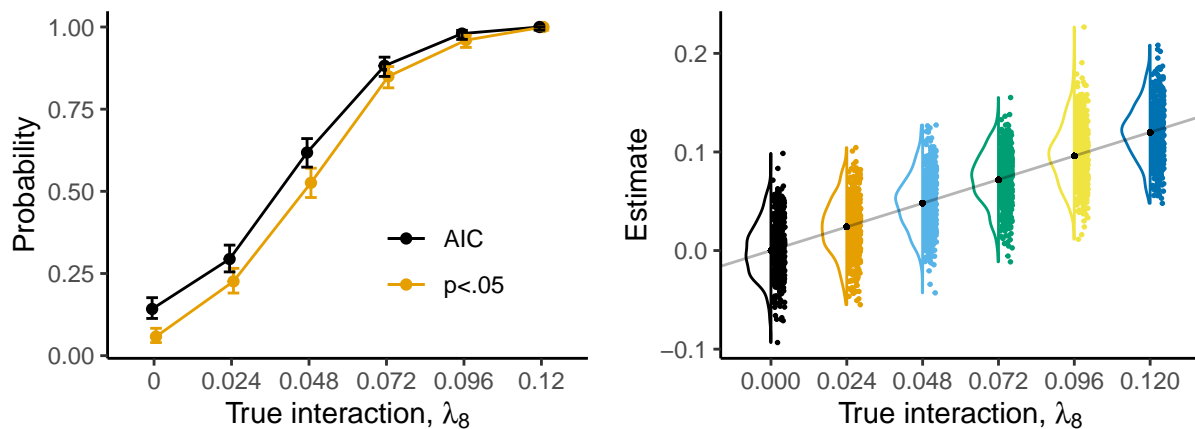


Figure 13: Left: Probability of selecting a model containing an interaction term as a function of the magnitude of the interaction. 'AIC' denotes Akaike information criterion and ' $p < .05$ ' denotes selection based on testing  $\lambda_8 = 0$  versus  $\lambda_8 > 0$ . Error bars show 95% confidence intervals. Right: Violin-dotplots (Hintze & Nelson 1998) of estimated interactions for different values of the true interaction. Gray line and black points indicate the true values, and colored points indicate estimates in single Monte Carlo samples. Values are based on 500 Monte Carlo samples for each parameter combination.

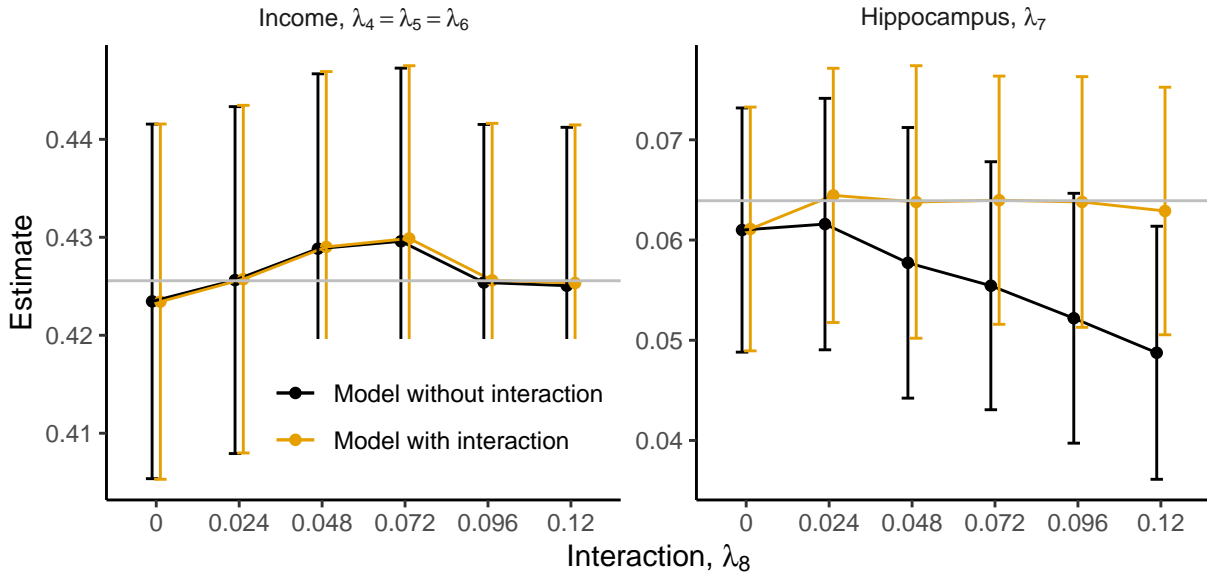


Figure 14: Estimated factor loadings in latent covariate model. Horizontal gray lines show the true values of the parameter, and error bars show 95% confidence intervals.

the model, the estimates had low bias and close to nominal coverage of confidence intervals, as shown in Figures 14 and 15. An exception was the effect of socioeconomic status on hippocampal volume  $\lambda_7$ , which was biased and had below nominal coverage in model (f) when the true interaction  $\lambda_8$  was large. However, in this case model (f) is misspecified, and as suggested by Figure 13 (left), the correct model (e) would be chosen with high probability. Finally, we investigated pointwise confidence intervals for lifespan trajectories at latent socioeconomic status equal to the mean or one or two standard deviations above or below mean, corresponding to the curves in Figure 4 of the main manuscript (right). As shown in Figure 16, the pointwise confidence intervals had close to nominal coverage, whereas the simultaneous confidence intervals in general were conservative, with coverage above 95%.

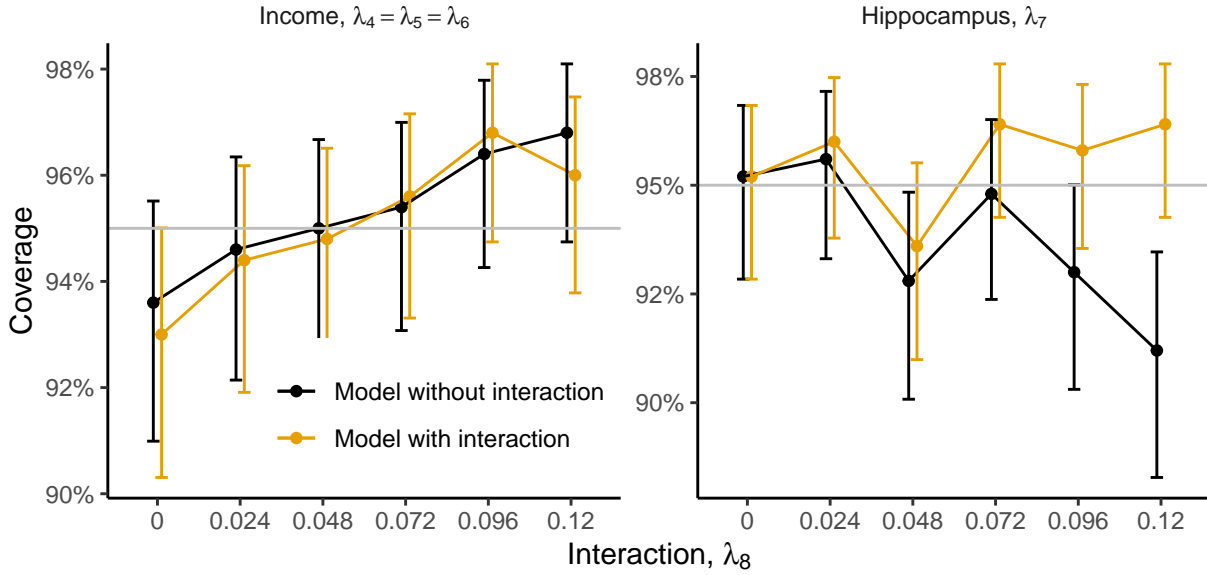


Figure 15: Actual coverage of 95% confidence intervals for factor loadings in latent covariate model. Horizontal gray lines show the 95% target value, and error bars show 95% confidence intervals.

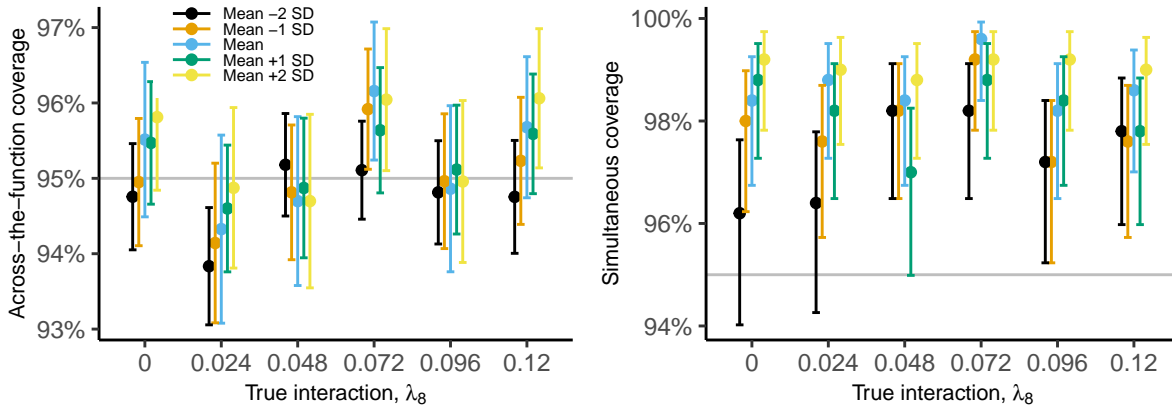


Figure 16: Across-the-function coverage of pointwise confidence intervals (left) and coverage of simultaneous confidence intervals (right) for five levels of latent socioeconomic status  $\eta_1^{(2)}$ . Intervals were computed with model (e), which contained a non-zero interaction term  $\lambda_8$ .



## References

- Arnold, J. B. (2021), ‘ggthemes: Extra themes, scales and geoms for ‘ggplot2’’. R package version 4.2.4.
- Bengtsson, H. (2021), ‘A unifying framework for parallel and distributed processing in R using futures’, *R Journal* .
- Genz, A., Bretz, F., Miwa, T., Mi, X., Leisch, F., Scheipl, F. & Hothorn, T. (2020), *mvtnorm: Multivariate Normal and t Distributions*. R package version 1.1-1.
- Hall, P. & Opsomer, J. D. (2005), ‘Theory for penalised spline regression’, *Biometrika* **92**(1), 105–118.
- Hintze, J. L. & Nelson, R. D. (1998), ‘Violin Plots: A Box Plot-Density Trace Synergism’, *The American Statistician* **52**(2), 181–184.
- Komsta, L. & Novomestky, F. (2015), *moments: Moments, Cumulants, Skewness, Kurtosis and Related Tests*. R package version 0.14.
- Meschiari, S. (2021), *latex2exp: Use LaTeX Expressions in Plots*. R package version 0.5.0.
- Newcombe, R. G. (1998), ‘Two-sided confidence intervals for the single proportion: Comparison of seven methods’, *Statistics in Medicine* **17**(8), 857–872.
- Parke, W. R. (1986), ‘Pseudo Maximum Likelihood Estimation: The Asymptotic Distribution’, *The Annals of Statistics* **14**(1), 355–357.
- Pedersen, T. L. (2020), *patchwork: The Composer of Plots*. R package version 1.1.1.
- R Core Team (2020), *R: A Language and Environment for Statistical Computing*, R Foundation for Statistical Computing, Vienna, Austria.

- Ruppert, D. & Carroll, R. J. (2000), ‘Theory & Methods: Spatially-adaptive Penalties for Spline Fitting’, *Australian & New Zealand Journal of Statistics* **42**(2), 205–223.
- Tiedemann, F. (2020), *gghalves: Compose Half-Half Plots Using Your Favourite Geoms*. R package version 0.1.1.
- Vaughan, D. & Dancho, M. (2021), *furrr: Apply Mapping Functions in Parallel Using Futures*. R package version 0.2.2.
- Vonesh, E. F. (1996), ‘A note on the use of Laplace’s approximation for nonlinear mixed-effects models’, *Biometrika* **83**(2), 447–452.
- Wickham, H. (2016), *ggplot2: Elegant Graphics for Data Analysis*, Springer-Verlag New York.
- Wickham, H. (2019), *stringr: Simple, Consistent Wrappers for Common String Operations*. R package version 1.4.0.
- Wickham, H. (2020), *tidyr: Tidy Messy Data*. R package version 1.1.2.
- Wickham, H., François, R., Henry, L. & Müller, K. (2021), *dplyr: A Grammar of Data Manipulation*. R package version 1.0.4.
- Wickham, H. & Seidel, D. (2020), *scales: Scale Functions for Visualization*. R package version 1.1.1.
- Wilson, E. B. (1927), ‘Probable Inference, the Law of Succession, and Statistical Inference’, *Journal of the American Statistical Association* **22**(158), 209–212.

# Supplement C: Case Studies

This document contains supplementary data for the case studies presented in Sections 3.2 and 3.3 of the main manuscript.

## 1 Factor-by-Curve Interaction Model

Figure 1 shows item responses to the digit span tests.

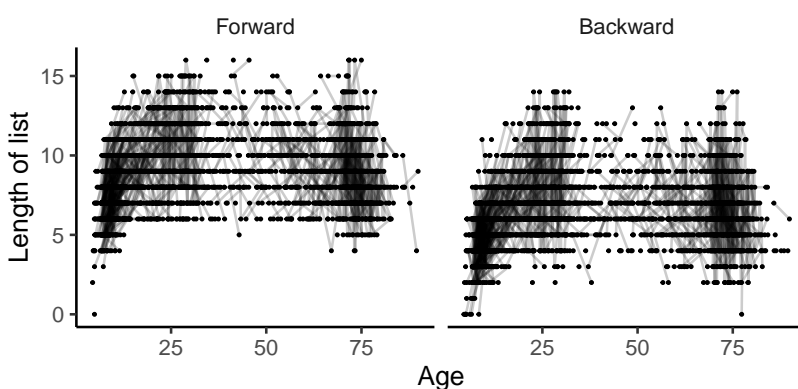


Figure 1: Observed responses to the digit span tests. Dots show individual responses, and black lines connect multiple timepoints for the same participant.

## 2 Latent Covariates Model

### 2.1 Model Selection

We compared models using the marginal Akaike Information Criterion (AIC). Since the models differed only in terms of the number of factor loadings, the degrees of freedom were appropriately defined as the number of fixed effect (Akaike 1974, Vaida & Blanchard 2005). Based on the results shown in Table 1 we chose model (f), with equal loadings for

the education items, equal loadings for the income items, and no interaction effect between age and socioeconomic status on hippocampal volume.

Table 1: Comparison of models for the effect of socioeconomic status on hippocampal volume. AIC values have been shifted to be zero for the full model, for ease of comparison.

Model	DF	Log-likelihood	AIC
(a): Free loadings	20	-5470	0.00
(b): (a) and no interaction, $\lambda_8 = 0$	19	-5471	-0.67
(c): Parents equal, $\lambda_1 = \lambda_2$ and $\lambda_4 = \lambda_5$	18	-5471	-1.28
(d): (c) and no interaction, $\lambda_8 = 0$	17	-5472	-1.91
(e): Item groups equal, $\lambda_1 = \lambda_2 = \lambda_3$ and $\lambda_4 = \lambda_5 = \lambda_6$	16	-5471	-5.18
(f): (e) and no interaction, $\lambda_8 = 0$	15	-5472	-5.84
(g): (f) and no main effect, $\lambda_7 = \lambda_8 = 0$	14	-5474	-4.56

'DF' denotes degrees of freedom.

## 2.2 Parameter Estimates

Table 2 shows item intercepts for the latent covariates model.

## References

- Akaike, H. (1974), 'A new look at the statistical model identification', *IEEE Transactions on Automatic Control* **19**(6), 716–723.
- Vaida, F. & Blanchard, S. (2005), 'Conditional Akaike information for mixed-effects models', *Biometrika* **92**(2), 351–370.

Table 2: Item intercepts in model of hippocampal volume and socioeconomic status.

Parameter	Estimate	SE	SE-naive	Units
<i>Item intercepts</i>				
Father's education, $\beta_{s1}$	2.81	0.00687	0.00687	log(years)
Mother's education, $\beta_{s2}$	2.81	0.00673	0.00673	log(years)
Education, $\beta_{s3}$	2.81	0.00542	0.00541	log(years)
Father's income, $\beta_{s4}$	13.2	0.0401	0.04	log(NOK)
Mother's income, $\beta_{s5}$	13.2	0.037	0.037	log(NOK)
Income, $\beta_{s6}$	13.1	0.0391	0.0385	log(NOK)